Whole genome regulatory effect of *MoISW2* and consequences for the evolution of *Magnaporthe oryzae*

Mengtian Pei[1], Yakubu Saddeeq Abubakar[2,3], Hina Ali[1], Lianyu Lin[1], Xianying Dou[1], Guodong Lu[1], Zonghua Wang[1,4], Ya Li[1*] Stefan Olsson[1,5*]

[1]State Key Laboratory of Ecological Pest Control for Fujian and Taiwan Crops, College of Plant Protection, Fujian Agriculture and Forestry University, Fuzhou 350002, China

[2]Key Laboratory for Plant-microbe Interaction, College of Life Sciences, Fujian Agriculture and Forestry University, Fuzhou 350002, China

[3]Department of Biochemistry, Faculty of Life Sciences, Ahmadu Bello University, Zaria 810103, Nigeria

[4]Institute of Oceanography, Minjiang University, Fuzhou, China

[5]Plant Immunity Center, Haixia Institute of Science and Technology, College of Life Science, Fujian Agriculture and Forestry University, Fuzhou 350002, China

*Correspondence:

Ya Li and Stefan Olsson

liya-81@163.com & Stefan@olssonstefan.com

Author contributions:

Mengtian Pei: ChIPseq and initial analyses; RNAseq and initial analyses; manuscript preparation and writing.

Yakubu Saddeq Abubakar: Constructive manuscript critique; manuscript corrections

Hina Ali: ChPseq; RNAseq

Lianyu Lin: Retrotransposon analysis of ChPseq data.

Xianying Dou: Constructive manuscript critique; manuscript corrections

Guodong Lu: Supervision; manuscript corrections

Zonghua Wang: Supervision; manuscript corrections

Ya Li: Obtaining funds; supervision; initial planning of experiments; construction of ISW2 mutant and phenotype analysis; manuscript preparation and writing

Stefan Olsson: ChIPseq and RNAseq extended analyses and synthesis; MEME, FungiFun, antiSMASH analyses; manuscript planning; manuscript preparation and writing.

Keywords: heterochromatin, epigenetics, nucleosomes, avirulence genes, retrotransposons, evolution

Abstract (words now 290) (can easily be shortened to 250 or 200)

Isw2 proteins are conserved in eukaryotes and are known to bind to DNA and dynamically influence local chromosome condensation close to the DNA binding site in an ATP-dependent manner making genes close to the binding sites more accessible for transcription and repression. A putative *MoISW2* gene was deleted with large effects on pathogenicity as a result, complemented and combined with a ChIP-sec to identify binding sites, RNAsec to test effects on regulation of genes along the chromosomes and compared with RNAseq from 55 downloaded RNA-seq datasets from the same strain. MoIsw2 binding and activities create regions of multiple binding sites with high gene expression variability close to the binding sites while surrounding regions have lower gene expression variability. We show that genes affected by the MoIsw2 activity are niche-determinant genes (secreted proteins, secondary metabolites and stress-coping genes) and avirulence genes. We further show that MoIsw2 binding sites coincide with known transposable elements (TE) making it likely that TE-transposition of the binding sites can affect the transcription profile of *M. oryze* in a strain-specific manner. We discuss that since avirulence genes are close to the MoIsw2 sites, TE transposition likely changes not just the expression and eventual silencing of the avirulence genes but the expression of a whole range of niche determinant genes. We conclude that MoIsw2 is a likely candidate for a master regulator that regulates the dynamic balance between biomass growth and nutrient uptake combined with reactions to the biotic and abiotic environment, i.e., the balance between anabolism and catabolism. Since TE transposition is known to be stress-induced the overall effect of TE activity together with MoIsw2 activity is likely to be a mechanism that creates more mutations and faster evolution of niche determinant genes than for housekeeping genes.

Introduction

The eukaryotic genome is organized into condensed nucleosomes, limiting access to DNA for transcription factors and more loosely packed regions that are easier to access for interactions with DNA for transcription factors and repressors. The cellular inheritance of this pattern is the basis of animal cell line specialization during embryogenesis (Serrano, Vazquez, and Tischfield 2013). Thus, DNA accessibility in fungi also plays an essential role in determining which genes can be efficiently transcribed (Huang et al. 2021).

Imitation Switch 2 (ISW2) belongs to the Imitation SWItch) subfamily (Uniprot) of the SNF2 (Sucrose Non-Fermentable)/RAD54 helicase family. ISW2 proteins contain a Myb/Sant domain close to their C-termini that binds DNA. A role as a transcription factor is the main role often implicated for the Myb-domain containing family proteins in eukaryotes and especially in plants (Wieser and Adams 1995; Mateos et al. 2006; Du et al. 2009; Dubos et al. 2010; Lin et al. 2011; 2012; Prouse and Campbell 2012; Ambawat et al. 2013; Pattabiraman and Gonda 2013; Kim et al. 2014; Baldoni, Genga, and Cominelli 2015; Dong et al. 2015; Liu, Osbourn, and Ma 2015; Roy 2016; Matheis et al. 2017; Valsecchi et al. 2017; Verma, Gazara, and Verma 2017; Allan and Espley 2018; Mitra 2018; Wang, Angelis, and Thein 2018; J. Li et al. 2019; Ma and Constabel 2019; Yunpeng Cao et al. 2020).

A true Isw2 should be involved in gene regulation by regulating the access to DNA for transcription factors and repressors through binding to DNA and controlling nucleosome positioning instead of being a classic transcription factor (TF) (Fazzio, Gelbart, and Tsukiyama 2005; Hada et al. 2019; Kagalwala et al. 2004). Generally, Isw2 has a histone binding domain that interacts with histone 4 of a nucleosome and a catalytic ATPase domain close to the N-terminus that reacts with ATP and change the Isw2 protein conformation (Whitehouse et al. 2007; Hota and Bartholomew 2011; Dang et al. 2014) so that the nucleosome moves towards the Isw2 DNA binding site (Fazzio, Gelbart, and Tsukiyama 2005), and in that way, transcription is regulated by changing TF and repressor access to DNA. Isw2 is thus involved in targeted nucleosome positioning around these sites. This regulation causes a localized nucleosome condensation that negatively affects the regulation of the genes at the DNA binding site (Whitehouse et al. 2007) but favors regulation a bit further away from it (Fazzio, Gelbart, and Tsukiyama 2005; Donovan et al. 2021).

There has been much research into this area, but it has become clear that *in vitro* mapping of Isw2 binding and nucleosome positioning does not reflect what mechanistically occurs *in vivo* (Fazzio, Gelbart, and Tsukiyama 2005; Donovan et al. 2021), or the very transient nature of the interaction with His4 (Erdel et al. 2010; Erdel and Rippe 2011). The nucleosomes closest to the Isw2 binding sites get dynamically locked by very frequent (seconds) interaction with the Isw2 protein in an ATP-dependent manner. The activity keeps the closest nucleosome(s) immobile, while nucleosomes at a further distance get more freedom to move. The accessibility for transcription/repression will then be limited at the *ISW2* DNA binding site while increasing but further away since the local nucleosome condensation creates an increased possibility of movements of the surrounding nucleosomes (Donovan et al. 2021). Experiments have shown that both the largest subunits of the Isw2 complex, Isw2, and Itc1, are needed for robust, target-specific binding to DNA while Isw2 alone is sufficient for basal level binding (Fazzio, Gelbart, and Tsukiyama 2005).

Furthermore, Isw2 is known to bind DNA preferentially at intergenic regions (Whitehouse et al. 2007) where transposable elements (TEs) are commonly located (TE target sites). These sites are staggered cut palindromic target sites (Linheiro and Bergman 2008). In addition, TEs are involved in stress adaptation and host specialization of the rice blast fungus *Magnaporthe oryzae* (Chadha and Sharma 2014; Yoshida et al. 2016) and should especially be needed when the host plant detects the fungus as a pathogen at the transition between the endophytic to necrotrophic infection phase of the fungus and thereafter (Yiyang Cao et al. 2022).

105 *ISW2* is highly expressed and often considered a "housekeeping" gene stably expressed under normal
106 conditions (Machné and Murray 2012). The stable expression of housekeeping genes has recently been
107 challenged, and many genes traditionally considered stably expressed are unreliable when expressed outside
108 relatively narrow conditions. Thus better methods for selecting housekeeping genes that better fit a specific
109 set of conditions or tissues have been employed (Stanton et al. 2017). On the other hand, the change in
110 ratios of target genes to housekeeping genes reflects the actual change in gene expression ratios of 2 genes
111 of interest. In a previous paper from our lab (Zhang et al. 2019), we used correlations of expression profiles
112 between genes of interest to probe possible gene functions. That can be done in transcriptomic data from
113 many labs and is especially useful if the calculations are done for all data and not just average value data.
114 Then, even the variation between replicates can be used to calculate the correlation between any two genes'
115 expressions since these ratios reveal the dependencies of one gene's expression on the other gene, or both
116 genes' expressions on a third. Using ratios of gene expressions can thus reveal putative gene functions and
117 help identify genes with specific putative functions that should correlate with the expression of well-known
118 orthologous genes (Zhang et al. 2019).
119
120 In this study we studied the putative *MoISW2* in *M. oryzae* as an *ISW2* gene that affects gene regulation
121 close to the MoIsw2 protein binding sites in the fungal genome. Deletion of the gene negatively affected
122 pathogenicity and stress tolerance. We further show that MoIsw2 binding is at TEs within the genome and
123 that genes close to the binding sites are more differentially regulated (up or down). The affected genes are
124 mainly niche-determinant genes; this, combined with TE transpositions, is a likely mechanism for biased
125 evolution (Monroe et al. 2022) in *M. oryzae* with a faster mutation rate for these genes.
126
127 **Results**
128
129 **Bioinformatics similarity and domain structure**
130 The protein encoded by the MGG_01012 gene is annotated as a putative MoIsw2 in the NCBI
131 database. From its N to C termini, Isw2 proteins consists of DExx, Helicase C, HAND, SANT and
132 SLIDE domains (Hopfner et al. 2012). Thus, the MoIsw2 protein is most probably an Isw2 protein
133 of the Iswi and Isw2 type (**Fig 1A**).
134
135 **Phenotypes of *ΔMoisw2* mutant and subcellular localization of the Isw2 protein**
136 The *MoISW2* gene was deleted in the *M. oryzae* Ku80 background strain and the deletion was
137 confirmed by Southern blot (**Fig S1**). The effect of this mutation on the vegetative growth of the
138 fungus was tested on three types of media namely complete medium (CM), minimal medium (MM)
139 and rice bran medium (RBM), after incubation at 28 ℃ for ten days. The assays showed
140 significantly decreased colony size of the mutant on all the three media when compared to the
141 background strain Ku80 and the complemented strain (*ΔMoisw2*/*MoISW2*) (**Fig. 1B**). A standard
142 panel of stress treatments added to the CM medium was used to test whether the deletion of the
143 *MoISW2* gene affected the fungal growth rates on different stressing media (Ya Li et al. 2014). The
144 CM medium without addition of any stress-inducing agent was used as the control medium. The
145 *ΔMoisw2* mutants are strongly inhibited by both SDS (which affects membrane integrity) and
146 NaCl (which induces osmotic and ionic stress) compared to the controls (**Fig. 1C)**, suggesting that
147 membrane pumps which depend on the membrane potential might not be necessarily upregulated
148 and working well in the mutant (Gostinčar et al. 2011). Furthermore, we tested the ability of the
149 mutant to produce conidia, which are essential inoculums for the spread of rice blast disease from
150 plant to plant in the field. We tested this by checking the abundance of conidiophores (which bear
151 conidia) in the various strains. It was discovered that while the WT and complemented strains
152 produced many conidiophores, each of which harbors more than one conidium, the *ΔMoisw2*
153 mutant only produced scanty conidiophores with very few conidia (**Fig. 1E**). Next, the *ΔMoisw2*
154 mutant was tested for pathogenicity on rice and barley leaves and compared with the Ku80
155 background strain and *ΔMoisw2*/*MoISW2* complemented strain**.** Since the *ΔMoisw2* mutant
156 produces too few conidia to be used as inoculum, agar plugs were used to infect healthy rice and

barley leaves in the infection assay. The assay showed no infection for the *ΔMoisw2* mutant strains (**Fig. 1D**). We reasoned that this could be due to an inability of the mutant to penetrate the plants cuticles. Therefore, we inoculated the fungal strains on aseptically wounded spots on the leaves and found that the *ΔMoisw2* mutant could not develop any obvious disease symptoms on the leaves, indicating that the *MoISW2* gene is needed for successful infection of rice or barley leaves **(Fig. 1D)**. From hyphae, *M. oryzae* can form appressoria needed for leaf infection. We found that appressoria formation was not affected by the *MoISW2* mutation, confirming that the cause of no infection in the infection assay was probably not a lack of appressoria formation (**Fig. 1E**). Finally, the Moisw2/*MoISW2-GFP* complementation was used to visualize the subcellular localization of MoIsw2. This was performed in a strain expressing Histon1-mCherry (RFP) (as a nuclear marker) because we expected that MoIsw2-GFP should accumulate in the nucleus as its orthologues do in other eucaryotes. Consistently, the MoIsw2 protein was observed to colocalize with the nuclear marker in hyphae, conidia and appressoria (**Fig. 1F**). Taken together, these results suggest that MoIsw2 directly or indirectly regulate genes encoding proteins that strengthen the cell wall and cell membrane barrier in several ways important for growth inside a plant and might explain why deletion of the gene decreased the pathogenicity of the fungus.

Correlation analyses of *ISW2* expression with expressions of nucleosome histones and ITC1

Histone 1 is involved in epigenetic activities, and its expression is linked to the silencing activity (Willcockson et al. 2021). The active Isw2 protein complex contains Itc1 and binds DNA and Histone 4 (Donovan et al. 2021). *HIS1* is also normally involved in epigenetic effects. We used published expression data from the course of rice leaf infection, from many different published experiments, to investigate correlations between genes for histones and the putative MoIsw2 in our strain. We have investigated such correlations of expression with identified genes a putative gene should interact with previously for other genes of the same Ku80 strain as we use in this paper (Guy 11) (Zhang et al. 2019). We used the same published data and method to investigate if the putative *MoISW2* is transcriptionally coregulated with genes that encode proteins MoIsw2 need to interact with to perform MoIsw2 local site-specific epigenetic activities. The *MoHIS1* expression increases steeply with *MoISW2* gene expression. The putative *MoISW2* is also found to be closest co-regulated with the putative *MoHIS4* in the downloaded data (**Fig. 2**). In *M. oryzae,* there are two genes (MGG_06293 and MGG_01160) predicted to encode an identical His4 protein that we call *MoHIS4a* and *MoHIS4b* genes, respectively, and the sum of these gene regulations should reflect the regulation of the MoHis4 protein. Isw2 works together with ITC1 in a complex that interacts with His4 (Kagalwala et al. 2004); thus, the expression of these 4 putative genes (*MoISW2*, *MoITC1* and *MoHIS4a+MoHIS4b*) producing 3 proteins (MoIsw2, MoItc1 and MoHis4) should be correlated in *M. oryzae,* and they are nicely correlated in the data from plant infection (**Fig. 2** and **Fig S2**). Thus, it would mean that the putative MoIsw2 is a real Isw2 as these proteins are known to interact with His1, Itc1 and His4 in a complex (Fazzio, Gelbart, and Tsukiyama 2005). The expression of *MoHIS2B* is related to the overall growth rate (Zhang et al. 2019) and is correlated with *MoISW2* but not with a steep slope, indicating that a smaller amount of MoHis2B is needed than His4 for handling the de novo DNA synthesis per cell than what is needed when Isw2 activity is high. Also, the expression of *MoHIS3* but not *MoHIS2A* is significantly correlated with the putative *MoISW2*. **(Fig. S3).** Although the MoIsw2 protein interacts directly with His4 such interactions could not be detected using a yeast two hybrid assay (data not shown) and the lack of positive results in this assay is likely due to the very transient nature of the interaction (Erdel et al. 2010; Erdel and Rippe 2011).

Thus, the putative *MoISW2* gene likely encodes a putative MoIsw2 protein involved in targeted local chromatin compaction working with MoHis1, MoItc1 and MoHis4 (Fazzio, Gelbart, and Tsukiyama 2005; Donovan et al. 2021; Willcockson et al. 2021). From now on, we skip "putative" as an attribute and investigate if MoIsw2 has the expected functions as an Isw2 and what other effects it has on the biology of the fungus. Also, the local and chromatin compaction caused by MoIsw2 should be dynamic and stronger the more the gene and the protein are expressed and the more ATP there is available for the dynamic interaction.

ChIP-seq analysis DNA binding motifs

We made a MoIsw2-GFP fusion protein to perform a ChIP-seq analysis to find conserved DNA binding palindromic motifs for the binding of MoIsw2 to *M. oryzae* DNA sequences.

As mentioned in the introduction, Isw2 proteins are known to preferentially bind DNA at intergenic regions where transposable elements (TEs) are commonly located (Whitehouse et al. 2007) with staggered palindromic motif target sites (Linheiro and Bergman 2008). TEs are mainly located intergenic in *M. oryzae* in previous unmapped DNA (Chadha and Sharma 2014; Bao et al. 2017) and appear to affect secreted protein expression differently in different *M. oryzae* strains (Bao et al. 2017).

Our new data showed hits mainly for intergenic sequences (**Supplemental Data 1**) where the palindromic retrotransposon sequences are preferentially located (Linheiro and Bergman, 2008). For these reasons, we looked for palindromic motifs in the ChIP-seq sequences interacting with MoIsw2-GFP. For this analysis we used the MEME website and as input all sequences (peaks). In addition, we also searched for previously identified RT sequences (Bao et al. 2017) in the ChIP-seq sequences

Three palindromic motifs were found to be common (**Supplemental Data 2**) with 47, 196 (**Fig. 2F)**, and 32 occurrences for motif 1, 2 and 3 respectively, located at 267 DNA locations, the large majority of these locations are intergenic. We investigated in detail the 196 hits and the majority of these hits were indeed intergenic (113), while the rest (63) were in the promoter region of a gene. Using a TOMTOM search at the MEME website, we found that the most common palindromic motif 2 is similar to a known Myb-binding protein containing a human DNA binding motif (**Fig. S4 Supplemental Data 3**).

MoIsw2 DNA binding and its influence on close-by avirulence gene expression.
Sub-hypothesis from the above observations: Transposable elements interacting with MoIsw2 may play a direct role in a pathogen-plant arms race if they affect the expression of the nearby avirulence genes (Chadha and Sharma 2014; Bao et al. 2017) through targeted nucleosome condensation (Bourras et al. 2016; Fijarczyk et al. 2022; Feurtey et al. 2023). For this function, these genes should preferably be adjacent to the MoIsw2 binding site, and their expression should be affected differently depending on their closeness to the binding site. Avirulence genes are often effectors the pathogen needs to efficiently cause disease and parasitize the host, but different cultivars of the host acquire resistance against these proteins naturally or through human exploitation in plant breeding programs to develop disease-resistant plant varieties (Jones and Dangl 2006).

To test this sub-hypothesis, we first made a list of all known avirulence genes noted for *M. oryzae* at NCBI (**Table 1**). There are 16 avirulence genes of different types and the avirulence cluster for cytochalasan-type compound biosynthesis (Collemare et al. 2008; Song et al. 2015) contains 12 more genes. The cytochalasan cluster is specifically activated at early hours post-infection (HPI) during penetration and produces a secondary metabolite recognized by the *R* gene *Pi33* in resistant rice cultivars (Collemare et al. 2008). Avr-PWL1 and Avr-PWL2 (Dioh et al. 2000), together with the previous, make 18 classic avirulence-type genes, excluding the cytochalasan gene cluster genes (**Table 1**). Most of the genes in the cytochalasan cluster are very close to the MoIsw2 palindromic DNA binding motif site, and several are differently expressed in Guy11 and 98-06 (**Table 1**), which might lead to the production of different final metabolites from the cytochalasan gene cluster even if the metabolites function as virulence factors.

Six other avirulence genes are not expressed in either strain (**Table 1**). Of these 6, half of the genes are close to the MoIsw2 binding site, and 3 are further away in Guy11. Two avirulence genes (MGG_17614 and MGG_15611) are in supercontigs with unknown gene order in our data, so it is unsure how far they are from a MoIsw2 binding site.

We searched the MoISW2 ChIPseq sequence data for described TEs and found TEs in and mapped the MoIsw2 binding sites to the genome as well as the position of all found transposable elements (TEs) (**Fig. 3**).

As can be seen the positioning of the MoIsw2 binding sites with the palindromic motifs are close to retrotransposons and the differential regulation and expression variation that likely affects indicate that MoIsw2-specific targeting is instrumental for stabilizing avirulence gene expression appropriately in relation to common local plant varieties and their resistance. This data and analyses with additional references are available in a supplemental file (**Supplemental data 4 and 5**).

The binding of MoIsw2 regulates the genes closest to the motif 2 binding sites

We next performed an RNAseq for the *ΔMoisw2* strain and the background *Ku80* strain, where we investigated the regulation of the genes with *MoISW2* ChIP-sequence DNA-binding hit in the promoter region or the gene closest to the most common found intergenic MoIsw2 motif and binding site (**Fig. 3AB**). There was a general upregulation of the genes closest to the MoIsw2 binding sites in the *ΔMoisw2* mutant (**Fig. 3A**). For these genes, the *ΔMoisw2*/*Ku80* expression ratio is lower when the MoIsw2 is predicted to bind directly in the promoter region than for the closest gene for a predicted intergenic binding of MoIsw2. On the other hand, if absolute (positive or negative) regulation was considered both types of genes, with MoIsw2 binding in the promoter region or intergenic, had similar absolute regulation indicating that many genes with MoIsw2 binding in their promoter region are repressed in *ΔMoisw2*. This suggests that without MoIsw2 activity, repressors can also get access to the DNA (**Fig. 3B**). These observations support MoIsw2 as an Isw2 protein that creates a local nucleosome condensation at specific nucleosomes (Donovan et al. 2021) affecting both genes' transcription and repression at slightly further distances from the DNA binding sites.

Overall functional classification of differentially expressed RNA-seq data

In *ΔMoisw2* grown on MM-medium, 339 genes were significantly upregulated relative to the background *Ku80*. The two largest significantly overrepresented gene categories were secondary metabolism and DNA-binding, while most other categories are related to DNA synthesis and DNA-pertaining activities and other growth-related processes (anabolism) (**Fig. 3C**). These are the genes MoIsw2 likely negatively regulates in *Ku80*. Most downregulated genes in the *ΔMoisw2* are genes involved in mitochondrial electron transport, other mitochondrial processes, transported compounds and other processes connected with uptake and respiration and oxidative phosphorylation (catabolism). In other words, our results indicate that MoIsw2 is involved in regulating the balance between anabolism and catabolism. Between DNA synthesis, which is safest without ATP generation by mitochondrial respiration since that generates Radical Oxygen Species (ROS), and oxidative phosphorylation, that is more effective in generating ATP from the metabolized substrates (Klevecz et al. 2004).

The local gene regulations close to the MoIsw2 palindromic DNA binding sites fit the Isw2-specific targeted DNA binding model.

DNA is wrapped around and slides around nucleosomes of similar sizes, with a constant overall Nucleosome Repeat Length (NRL) (van Holde 1989; Cutter and Hayes 2015; Donovan et al. 2021; Willcockson et al. 2021) and NRLs sizes vary slightly depending on the organism, cell type and cell status (van Holde 1989).
To further investigate local regulation around at or close to the binding sites with the found palindromic motif, we investigated our RNAseq data and ordered the MGG-codes for the genes in the order of the genes on the chromosomes (Chromosome order downloaded from BROAD).

Dynamic changes to chromosome packing should result in changes in regulation between experiments in the downloaded data. If MoIsw2 activity is responsible for these changes there should be the greatest variation in expression between experiments for genes positioned close to the MoIsw2 binding sites in the DNA. We tested this by plotting the variation of the measured gene expression responses in our RNAsec data and compared expression responses (positive and negative) in Ku80 (background) strain with the *ΔMoisw2* mutant strain (DelR). We could then test if the variation in expression responses (positive and negative)

(VarR) in the downloaded data from 55 RNAsec datasets from several labs shows expression variations at similar positions in the data. We found that the two gene expression variation measures were Log-Log correlated (P=5.3E-196) and that the response slope of the correlation was 0.56 with VarR on the x-axis (**Fig. S5**). We further calculated the distance between each gene and the closest MoIsw2 binding site and plotted that together with plots of the gene expression variation from our experiment (DelR) and the one from the downloaded data (VarR). In the plot (**Fig. 4**), we also included the positions of the avirulence genes. From these comparisons, one can see that gene regulatory responses along the genome are dependent on MoIsw2. Further we can identify regions along the DNA with high variation and close (less than 16 genes from the closest motif) to MoIsw2 binding motifs (A-U **Fig. 4**) and regions with less variation further away (17-to about 500 genes) from the MoIsw2 binding motifs (1-15 **Fig. 4**). In **Figure 4** we have marked the positions of the Avir genes as well.

For typical housekeeping genes like the ribosomal genes their expression depends on the overall rate of translation and should be quite constant between experiments. The ribosomal are mainly found further away from MoIsw2 binding sites and TEs confirming that the ribosomal proteins are in regions with more stable expression responses (**Fig. 5A**).

On the other hand, genes that are important for interaction with the environment as the secreted proteins with identified domains (SP) and smaller other secreted proteins (OSP) are positioned in the more variable genomic regions closer to the MoIsw2 binding motifs (**Fig. 5B** and **5C**)

Other genes that are important in interaction with the environment are secondary metabolites. Instead of searching the literature, we used the AntiSmash web server and submitted the whole DNA sequence from BROAD to get a list of core secondary metabolite genes. We found 64 such genes and plotted their positions along the ordered gene positions (**Fig. 6A**) and found that they are mainly positioned close to MoIw2 binding motif sites.

Epigenetic silencing can if it is persistent from generation-to-generation result in the silenced genes accumulating deleterious mutations since the genes are never expressed and needed in the ecological niche the organism lives in. We consider genes not expressed in any of the downloaded RNAsec datasets as potential pseudogenes (PP). Since the misuse of the pseudogene term does not make sense, we follow the nomenclature suggested (Cheetham, Faulkner, and Dinger 2020) and only use the term pseudogene alone for sequences that look like genes and are not expressed at all under natural conditions. Consequently, due to limited knowledge of most microorganisms' natural lifecycles, it is difficult to definitively classify a gene as a vestigial gene or a pseudogene. However, if a gene is rarely expressed under natural evolutionary relevant circumstances and accumulates mutations over time rendering it non-functional, it may eventually become a pseudogene. Several genes close to the *MoISW2* binding sites were not expressed at all in any of the 54 downloaded RNAseq datasets (**Supplementary Data 4**) (**Fig. 6B)** indicating that these genes could be or become vestigial genes or pseudogenes without biological roles, thus we call them potential pseudogenes. Since the misuse of the pseudogene term does not make sense, we follow the nomenclature suggested (Cheetham, Faulkner, and Dinger 2020) and only use the term pseudogene alone for sequences that look like genes and are not expressed at all under natural conditions. Consequently, due to limited knowledge of most microorganisms' natural lifecycles, it is difficult to definitively classify a gene as a vestigial gene or a pseudogene. However, if a gene is rarely expressed under natural evolutionary relevant circumstances and accumulates mutations over time rendering it non-functional, it may eventually become a pseudogene. Our observation that these genes are or have become potential pseudogenes during evolution is exciting since some of these genes close to the MoIsw2 binding sites are annotated as avirulence effector genes (**see Table 1**). The data and analyses behind the table and the next section are available in a supplemental file (**Supplemental Data 4**).

DNA binding genes

Since 65 genes were classified as DNA-binding and were among the enriched genes upregulated in *ΔMoisw2* (**Fig. 3C**) these could be conventional TFs, suppressors or other DNA binding genes

needed when interacting with the biotic and abiotic environment potentially of high importance during pathogenesis.

The 12 DNA-binding genes most suppressed by MoIsw2 activity are mainly involved in DNA repair (**Table 2**) needed for DNA synthesis and growth. Further pointing to that MoIsw2 affects balance between genes necessary for reacting to the environment and genes necessary for growth. Among the most regulate genes were two TFs and several helicases and genes needed for DNA repair. A fungal specific gene involved in (sexual) sporulation is also in this list of 12 DNA-binding genes most suppressed by the MoIsw2 activity.

Functional classification of genes potentially affected by the presence of MoIw2

A. At MoIsw2 binding sites in DNA sequences

We have above shown that genes under *MoISW2* control that are more expressed in the background *Ku80* strain compared to the *ΔMoisw2* strain are enriched for gene classes associated with secondary metabolism and biomass growth (anabolism) while the genes that are downregulated in the mutant are connected to aerobic metabolism and stress (**Fig. 3C**).

For the *MoISW2* ChIP-seq data, we investigated the FunCat classification of all genes adjacent to or in ChIP sequence hits to find out what types of genes are regulated and which are not. First, we removed double ChIP peak sequence hits close to the same gene so as not to count the same gene twice. We then investigated the list of genes that are closest to the MoIsw2 binding. These genes should be targeted by MoIsw2 and might be under positive or negative control from MoIsw2. According to the previous analysis, they should not belong to growth (anabolism) but be genes active when oxygen is consumed, and the substrates oxidized (catabolism) (Klevecz et al. 2004; Machné and Murray 2012). In addition, the binding sequences are located close to avirulence genes and retrotransposons, so their regulation can shift depending on retrotransposon transpositions. Since ChIP-seq only shows potential binding to DNA *in vitro,* we cannot say if these genes are up or downregulated; only that regulation influenced by MoIsw2 is possible. Genes with ChIP binding hits closest to the MoIsw2 palindromic DNA binding motif site are mainly enriched for genes involved in secondary metabolism and other gene classes important for biotic interactions (**Fig. 7A)**. In contrast, categories of genes for biomass growth and housekeeping (anabolism) are depleted (**Fig. 7B**).

Other genes with ChIP-seq sequences could be affected. These genes are many more than those closest to the MoIsw2 palindromic DNA motif2 sites. For these, we find more gene classes (**Fig. 7A**), including detoxification and signaling (cyclic nucleotide-binding), disease, and defense, and these are all important gene classes involved in biotic and abiotic interactions with the environments. Depleted are gene classes characteristic for anabolism (biomass growth) (**Fig. 7B**).
Finally, the genes in the ChIP-seq data but not with motif2 hits (not containing the MoIsw2 palindromic DNA binding motif 2 site) are again genes enriched for secondary a genes and again genes involved in abiotic and biotic interactions. Genes needed for biomass growth are depleted (**Fig. 7C**).

Functional classification of the 500 genes showing the highest VarR and DelR, VarR values, and DelR values

As we have seen above (**Fig. 5 and 6**) the genes close to MoIisw2 binding motif123 are in general more variable expressed DNA regions between RNAsec plant infection experiments (VarR). These regions number the most TEs and core secondary metabolite genes. To get more information on functional classes regulated we used FungiFun again and did a functional classification of the 500 most variable genes (VarR) in the downloaded data and compared that with the genes most affected by the *MoISW2* deletion.

None of these genes are probably directly regulated by MoIsw2 but their access to gene regulation should be affected. Furthermore, similarities and differences between VarR and DelR should point to regulations biased for plant interactions or plate growth respectively.

Genes categories needed to cope with the abiotic and biotic environment are enriched among the 500 with the highest VarR and DelR values indicating that both the lab and inside plants' similar gene functions are in principle affected by the MoIsw2 activities. Depleted functional gene classes are growth-related genes (anabolic) and some stress-related genes. Genes categories needed to cope with the abiotic and biotic environment are again enriched among the VarR 500 most differentially regulated gene classes. Depleted are again growth-related genes (anabolic) and stress-related gene classes. The fungal biomass had recently been shifted from stationary (agar plugs) with the nuclei in various states of growth to a liquid medium for 48h triggering vigorous growth. Thus, variations are expected in how fast the biomass reacts to the new situation of plenty of nutrients, also among genes not affected by MoIsw2 activities. That is probably why unfolded protein response genes are differentially regulated. But in general, the gene functional classes in VarR alone and DelR alone are similar.

The differential regulation of transcription and translation between treatments during plant infection (VarR-specific) are genes that are expected to be genes responding in fungal-innate immunity (Ipcho et al. 2016) (reacting to plants in this case) and are further discussed in the discussion section. The DelR-specific enriched gene classes indicate fast aerobic growth of hyphal biomass in and nutrient uptake from the environment *in vitro*.

Discussion

Deletion effects on phenotypes, and on regulation (DelR) compared with variability in regulation between RNAseq experiments (VarR).

When *MoISW2* is deleted, the general growth of the fungus (**Fig. 1**) was negatively affected, as was the sensitivity to SDS and NaCl. Conidiation was completely abolished as was also pathogenicity, and the MoIsw2-GFP fusion accumulates in the nucleus as expected. The strong effect on infection and the fact that Isw2 proteins are known to affect the regulation of many genes in genomes through local chromosomes around several DNA binding sites (Fazzio, Gelbart, and Tsukiyama 2005) indicates that *MoISW2* could be a "master regulator" for regulating the many fungal defenses against the plant defenses since these and virulence factors (for example secondary metabolism) are upregulated in the biotrophy/necrotrophy transition and during the necrotrophic stage (Andrew et al. 2012; Kou, Qiu, and Tao 2019) when membrane effects on the pathogens are especially prominent and the fungus have to deal with plant ROS defenses.

We found that potential effector gene classes like avirulence genes, secreted proteins, and core secondary metabolite genes are located in the DNA regions that appear to be under MoIsw2 control supporting its role as a master regulator of gene access to genes necessary for reacting with the biotic and abiotic environment (**Fig. 5, 6, 7A**) are close to regions that are differentially regulated in the *ΔMoisw2* compared to the background K80 (DelR). These are also the same regions with the highest variability between experiments in a set of RNAseq data from 55 downloaded RNAseq datasets from experiments in planta (**Fig.5**) (VarR).

The overall regulation effect of all genes VarR and DelR of all genes in the two datasets were correlated as they should be if the regions in the two datasets are the same and strain specific and ot experiment specific and dependent on the organisation of chromatin in the particular strain. Growth inside a plant is stressful for a plant pathogen. The fungus must compete with the plant for all nutrients during the biotrophic stage without revealing its existence and then trigger plant immunity responses that it has to handle in the necrotrophic stage (Andrew et al. 2012; Chowdhury, Basu, and Kundu 2017; Rajarammohan 2021). When shifting to the necrotrophic stage the pathogenic fungus must thus both overcome plant defenses and nutrient limitations since when spreading inside the plant, nutrient limitations might occur (Josefsen et al. 2012). In support of a strain specific "master regulator" function regulating responses to environmental condition, we find that many fungal defence and virulence-related functional gene classes are regulated in the variably regulated chromosomal regions that appear to be under MoIsw2 activity control (**Fig. 8 and 9**). There is also a difference in the regulation of avirulence genes between *M. oryzae* strains and these genes are situated close to the MoIsw2 binding sites in the DNA giving the strain specificity of the "master regulator" function further support (**Table 1**)

474 **Regulation of chromatin condensation by nucleosome positioning**
475
476 **MoIsw2 is a true Isw2**
477 Direct interactions with His4 could not be detected by a yeast two-hybrid assay. The yeast Isw1
478 and Isw2 interactions with His4 are transient (approximately 200 and 80 bindings per minute,
479 respectively) and need a continuous ATP supply (Tsukiyama et al. 1999). Similarly, the interaction
480 in human cells has been measured in vivo using advanced microscopy and spectroscopy
481 techniques and found to be transient (10-150ms)(Erdel et al. 2010; Erdel and Rippe 2011). Thus, our
482 attempts to detect an interaction between MoIsw2 and MoHis4 using the yeast two-hybrid method
483 were unsuccessful, likely due to the transient nature of Isw2 interactions with His4.
484 On the other hand, the expression of MoIsw2 and the expression of orthologues to genes in
485 *M. oryzae* that an Isw2 protein are known to physically interact and form a functional Isw2 protein
486 complex (Donovan et al. 2021) are correlated (**Fig. 2**). That indicate that MoIsw2 is a true Isw2 with
487 a conserved Isw2 protein function and conserved order of domains in the protein (**Fig. 1A**)
488
489 **Regulation of MoIsw2 activity and regulation by *MoISW2* expression**
490 Isw1 translocate nucleosomes away from other nucleosomes, while Isw2 does the same towards
491 the center of DNA pieces and other nucleosomes *in vitro,* with the nucleosomes bound to
492 relatively short DNA pieces (Kagalwala et al. 2004; Zofall, Persinger, and Bartholomew 2004). It does
493 so also *in vivo* where it was found that Isw2 is mainly involved in the targeted regulation of DNA
494 around the Isw2 DNA binding site (Fazzio, Gelbart, and Tsukiyama 2005), as we also find (**Fig. 4,**
495 **Table 1**). Thus, the regulation of genes adjacent to the DNA-binding site is likely to be highly
496 dependent on ATP availability and competition for ATP in the cytoplasm-nucleus compartment.
497 ATP generation from fermentation is much faster but less efficient than from oxidative
498 phosphorylation when glucose is available. In yeast, growth is characterized by DNA replication,
499 mainly without mitochondrial oxidative activity (aerobic glycolysis), most probably to protect
500 DNA from mutations (Klevecz et al. 2004). In *M. oryzae,* MoIsw2 could thus be an ATP-regulated
501 switch (Machné and Murray 2012) between fast aerobic glycolysis, DNA-synthesis growth with
502 quality control, and slower but more efficient oxidative phosphorylation growth with high ATP
503 yield, oxidative defenses, and interaction with the abiotic and biotic environment that makes up
504 the *M. oryzae* ecological niche. Supporting this, we found that genes upregulated in the *ΔMoisw2*
505 mutant and thus repressed by MoIsw2 under other more ATP-limited aerobic growth conditions
506 are involved in fast growth and DNA synthesis, DNA quality control, while downregulated genes
507 in the mutant were those involved in oxidative phosphorylation, stress management, and
508 secondary metabolite biosynthesis (**Fig. 3EF** and **Table 2**).
509 As expected, the genes closest to the two central nucleosomes to the MoIsw2 DNA-binding
510 sites are downregulated in the background *Ku80* (Donovan et al. 2021), and when *MoISW2* is
511 deleted, such genes are upregulated (**Fig. 3A**).
512
513 **Regulation by MoIsw2 is dependent on distance from the MoIsw2 DNA binding sites.**
514 Gene regulation variability in the *ΔMoisw2* mutant strain compared to the background Ku80 strain
515 (DelR) as well as the variation between RNAseq experiments (VarR) are dependent on the
516 distance from the MoIsw2 DNA binding motif sites (**Fig. 5**). That agrees with that regulation is a
517 consequence of the MoIsw2 positioning of the closest nucleosomes giving more sliding space to
518 surrounding nucleosomes (Donovan et al. 2021) and consequently increased DNA access. Genes
519 affected by the MoIsw2 activities and being physically close to the palindromic binding sites in
520 the DNA are for example genes for secreted protein while core secondary metabolites while
521 typical housekeeping genes like genes encoding ribosomal proteins are further away (**Fig. 6**). In
522 support of this we found that the 500 most regulated genes (High VarR and/or DelR) with most
523 variable gene expression were significantly enriched for functional gene classes needed to react to
524 the biotic and abiotic environment and depleted for typical housekeeping genes (**Fig. 9**).
525 Interestingly, and in line with this interpretation the 500 genes specifically upregulated in VarR
526 (during plant pathogenesis) and in DelR (growth in vitro) are genes that reflects the two different

527 biotic/abiotic environments for the fungus. The functional gene classes specially enriched in VarR
528 are those that are expected for fungal innate immunity (Ipcho et al. 2016) and innate immunity that
529 is known to trigger very fast transcriptional responses (**Fig. 10**) (Smale 2012).
530
531 **Conserved and variable DNA**
532 Our observations suggest that the *M. oryzae* genome is organized into regions with constant
533 expression and variable expression depending on the environment. The regions with variable
534 expression are close to MoIsw2 DNA binding sites and contain genes important for the interaction
535 with the environment (biotic and abiotic) while regions with less variable expression contain
536 housekeeping genes. Such a division of the fungal genome into regions of housekeeping genes and
537 niche-determinant genes is consistent with previous findings in the relatively closely related
538 *Fusarium graminearu*m (Zhao et al. 2014).
539 Palindromic sequences are characteristic of retrotransposons that are mainly positioned
540 close to stress-related genes and avirulence genes in the genomes of fungal plant pathogens.
541 Fungal avirulence genes are plant-pathogen effectors that trigger different plant immunity
542 responses depending on plant variety and the basis for plant cultivar-specific resistance to specific
543 pathogen strains (the gene-for-gene relationship) (Bourras et al. 2016) and we find them close to
544 MoIsw2 binding motifs (**Table1, Fig5**). The *MoISW2* DNA binding sequences (the ChIPseq
545 sequences) also contained palindromic DNA motifs characteristic for most of the identified TEs
546 (Bao et al. 2017) (**Fig. 4**). A palindromic DNA motif gives genetic instability to the genome at the
547 site of the motif (Ganapathiraju et al. 2020; Svetec Miklenić and Svetec 2021). Stress, virulence, and
548 stress-related genes are in *M. oryzae,* also linked to transposable elements (Yoshida et al. 2016) and
549 we see this in our study as well (**6, 7A, 8-10**).
550 Different mutation rates or mutation bias of genes have recently been described as a new concept for
551 the plant *Arabidopsis thaliana* (Monroe et al. 2022). Genes with higher mutation rates are involved in biotic
552 and abiotic interactions. The gene found with the highest mutation rate was a gene responding to chitin,
553 which is present in symbiotic (pathogenic and nonpathogenic) fungi and insects (Monroe et al. 2022).
554 Transposable elements tend to accumulate in genomes and expand the genome with repetitive sequences
555 (Fijarczyk et al. 2022; Feurtey et al. 2023) unless there is some evolutionary constraint against such
556 expansion (Kremer et al. 2020; Fijarczyk et al. 2022). Phosphorous availability is a possible constraint
557 (Ågren, Wetterstedt, and Billberger 2012) since a considerable amount of the cell phosphorous, especially, is
558 bound up in DNA and not available for other purposes (Berdalet, Latasa, and Estrada 1994). Fungal plant
559 parasites can get phosphorous directly from their plant hosts by degrading the plant tissue and are not so
560 restricted by limited resources in the soil (Ågren et al., 2012). Thus plant parasites should be expected to
561 have more retrotransposons to adapt better to plant resistance and thus have relatively large genomes, as
562 they have (Fijarczyk et al. 2022; Feurtey et al. 2023). Endophytic fungi that have to coexist with their host in
563 their life cycle, and thus have to compete with the host for phosphorous, should, in consequence, have
564 smaller genomes, as they seem to have (Fijarczyk et al. 2022).
565 Our results show changes in regulating the avirulence genes between two *M. oryzae* strains
566 with different pathogenicity to different rice cultivars (**Table 1**). In addition, we did not detect any
567 expression for some putative avirulence genes close to the MoIsw2 DNA binding sites, which
568 suggests that those genes may be potential pseudogenes in these strains. That might indicate a
569 retrotransposon-aided genetic evolution of inherited epigenetic changes to regulation in reactions
570 to the environment (resistance of the plant cultivar). A regulation that can be genetically fixed,
571 first through loss of possible regulation (making genes into pseudogenes), and much later
572 complete gene loss or change of the potential pseudogenes so they cannot be easily recognized as
573 genes is a mechanism that potentially can result in a "biased" faster evolution (Chadha and Sharma
574 2014). Most of the potential pseudogenes (not expressed under any conditions reported in this
575 paper) were close to the MoIsw2 DNA binding sites with palindromic motifs supporting this
576 hypothesis for mechanism involving MoIsw2 activity in creating pseudogenes and completely
577 remove genes by making then unrecognizable as genes through mutations. That is if the ecological
578 niche does not change fast like it does for a plant pathogen because of efforts for resistance

breeding the susceptible plant, then the silenced genes can be fast become re-activated again by TE repositioning.

Our results further indicate that *MoISW2* regulates a switch between fast glycolytic growth and slower nutrient efficient aerobic stress-characterized growth, coping with abiotic and biotic stresses or, in other words, niche fitness. The loss of *ISW2* function in a unicellular Eukaryote or the early stages of fungal growth from a spore should make the fungus unfit for survival in a natural environment and become more dependent on aerobic fermentation for ATP synthesis that is not substrate efficient although generates ATP at a very high rate although inefficient (Pfeiffer and Morley 2014; Desousa et al. 2023). However, a limitation for eukaryotic cell to only aerobic fermentation could lead to uncontrolled cell growth and oncogenesis in a long-lived multicellular organism (Desousa et al. 2023), as ATP and fermentable nutrients can be received from surrounding cells and other tissues through the blood circulation. Mutations of the genes *SMARKA2* or *SMARKA4* that encode Brm and Brg1 proteins that are orthologues of fungal Swi2/Snf2 involved in nucleosome positioning in a way that has similarities to the nucleosome movements Isw2 can cause cancer (Reisman, Glaros, and Thompson 2009; Mittal and Roberts 2020; Yanan Li et al. 2021).

But a general shift to aerobic glycolysis and fast upregulation (within a few hours) of innate immunity-related genes associated with tissue inflammation is characteristic of fast defense against microbes through fast iron uptake, antimicrobial peptide production, and other responses needing rapid translational responses, as shown for *Fusarium graminearum* is general for eukaryotes (Ipcho et al. 2016). Such fast upregulated innate immune response in plants can be inhibited by fungal immune inhibitors acting on translation like trichothecenes the same fungus produces (Toyotome and Kamei 2021), most likely to attenuate immune responses in the plants it infects. In line with a fungal innate immunity scenario (Ipcho et al. 2016), genes involved in RNA synthesis and RNA processing were found to be upregulated in the *ΔMoisw2* mutant (**Fig. 3C**).

Is retrotransposon shifting *MoISW2* binding creating and directing the mutation bias by adapting the fungus to new challenges?

MoISW2 is likely an important player in a mechanism aiding both mutation bias and adaptation to new circumstances whose combined activities lead to natural adaptation-directed fast evolution (NADFE), a new concept that is similar to artificial adaptation-directed fast evolution that can be performed in a laboratory (Packer and Liu 2015). Since transposons DNA containing MoIsw2 palindromic DNA binding sites seems necessary for MoIsw2 activity, stress-activated transposon activity, known for creating genomic instability, can together with the MoIsw2 activity create a new adaptive regulatory landscape (Chadha and Sharma 2014) that can be stabilized relatively quickly and lead to mutation bias (Monroe et al. 2022). It could in addition be a possible mechanism sought after for a Lamarckian-Darwinian synthesis to help explain the fast evolution of new traits requiring many combined mutations that cannot be reconciled within Darwinian evolution strictly based on random mutations creating variation together with sexual recombination and natural selection favouring the better fitted variant (Bard 2011). The chance of multiple mutations that only together can become positive is theoretically much more likely to happen with NADFE, creating a mutation bias (Monroe et al. 2022). *ISW2* activities in eukaryotes could thus be one of the needed mechanisms to reconcile Lamarckian evolution with Darwinian evolution to bring about both the observed direction and the needed speed of evolution of specific traits when new niches become available, or there are drastic niche changes (Bard 2011).

Perspectives for future research

Evolution of the plant-pathogen interaction: The effect of exposing *M. oryzae* strains to different MoIsw2 activities and retrotransposon activities on the rate of genetic adaptation to a shift in rice cultivar is a possible future topic that could be exploited to understand how the pathogen adapts to different resistant cultivars and break plant resistance.

Agrochemicals: Searching for potential agrochemicals to manipulate MoIsw2 activities on His4 and DNA-binding is tempting since *MoISW2* is crucial for plant pathogenicity. Though MoIsw2's close resemblance to mammalian proteins with the same function indicates that such chemicals are likely negatively affecting orthologue proteins in mammals and might be cancerogenic to humans

632 since even small mutations in ISW2 orthologues in mammals can cause cancer (Reisman, Glaros,
633 and Thompson 2009; Mittal and Roberts 2020).
634 **Histon4:** Finally, we found 2 *MoHIS4* genes with large difference in DNA sequences (gene
635 duplication many generations ago) predicted to encode for identical proteins but differently
636 regulated and it seems like *M. oryzae* needs both genes (**Fig. 2**). This fact is of interest since His4
637 in nucleosomes is what MoIsw2 is supposed to interact with (Tsukiyama et al. 1999), and *HIS4*s are
638 examples of genes with the highest degree of purifying evolution (Piontkivska, Rooney, and Nei 2002).
639 We have thus started new research into the roles and regulation of these two *MoHIS4* genes and
640 how their regulations shift with growth conditions. Their predicted identical amino acid sequences
641 indicate that they are evolutionarily constrained to differ only by synonymous mutations.
642 Gene variability in expression: The most interesting genes for biotic and abiotic interactions are
643 also the genes with highest variability between experiments (VarR) creating problems when
644 estimating effects of manipulation with these genes. The common practice of only using 3
645 replicates for measuring effects on genes (like deletions) is probably not enough and we might
646 need to increase them to 5 or even more so we also can detect what type of distribution there is for
647 the gene expression of that gene. Strict normal or lognormal distribution is maybe only true
648 mainly for housekeeping genes.
649
650 **Consequences of MoIsw2 functions that are positive for the fungus's ability to stay pathogenic:** 1. The
651 MoIsw2 function will result in adaptive silencing of virulence/avirulence genes without gene loss due to
652 mutations of the actual DNA nucleotides. In other words, virulence genes are not quickly lost from the
653 adapted strains but can be called upon again if the available hosts change their resistance in the classical
654 gene-for-gene scenario (Flor 1956). 2. Adaptive silencing of virulence genes often found close to
655 transposable elements (Menardo et al. 2017) will lead to biased fast gene evolution of especially genes
656 involved in biotic interaction (Monroe et al. 2022) as in the gene-for-gene concept and is a possible
657 mechanism behind the speedy appearance of virulent pathogen strains capable of attacking newly developed
658 resistant plant varieties (Palloix, Ayme, and Moury 2009; Menardo et al. 2017).
659
660
661
662 **Materials and Methods**
663
664 **Fungal strains and media**
665 *Magnaporthe oryzae* B. Couch anamorph of the teleomorph *Pyricularia oryzae* Cavara was used for this
666 research. As background strain, we used Ku80 (generated from the WT strain 70-15) to minimize random
667 integration events when transformed (Villalba et al. 2008). The susceptible Indica rice (cv. CO-39) and
668 barley (cv. Golden Promise) used for the fungal pathogenicity tests were from the seed bank of our
669 laboratory. For both ChIP-seq and RNAseq, the strains used were grown and harvested similarly.
670
671 **Knockouts, complementations, and verifications**
672 The *MoISW2* is a *MYB* gene and *MYB* gene deletion vectors were constructed in the plasmid pBS-HYG by
673 inserting 1 kb up- and down-stream fragments of the target gene's coding region as flanking regions of the
674 HPH (hygromycin phosphotransferase) gene (H. Li et al. 2012). No less than 2 μg of the deletion vector
675 DNA of the target gene was introduced to Ku80 protoplasts, and transformants were selected for
676 hygromycin resistance to perform gene deletion transformations. Southern blotting was conducted to
677 confirm the correct deletion using the digoxigenin (DIG) high prime DNA labelling and detection starter Kit
678 I (11745832910 Roche Germany). The *MYB* gene complementation vectors were constructed by cloning the
679 entire length of the target gene with the native promoter region (about 1.5-kb) to the pCB1532 plasmid.
680 When making the complementation vector, GFP was linked to the C-terminal of the target genes to study the
681 sub-cellar localization of Myb proteins. The constructed vector DNA was introduced into the mutation
682 protoplast for gene complementation, and resulting transformants were screened using 50 μg/ml
683 chlorimuron-ethyl to select successful complementation strains. Detailed fungal protoplast preparation and
684 transformation methods have been described previously (H. Li et al. 2012). All primers needed for the

knockout and complementation are listed (**Table S1**). The sub-cellar localization of Myb proteins was observed by confocal microscopy (Nikon A1). GFP and RFP excitation wavelengths were 488 nm and 561 nm, respectively.

Colony and growth phenotype measurements

Vegetative growth was tested by measuring the colony diameter after ten days of growth in 9 cm Petri dishes at 25℃ under 12h-to-12h light and dark periods. Conidia production was evaluated by flooding the 12-day-old colony with double distilled water, filtering out the mycelia with gauze, and counting the conidia using a hemacytometer. The conidiophore induction assay was performed by excising one thin agar block from the fungal colony and then incubating it in a sealed chamber for 24 h with constant light (67). Mycelia appressoria were induced by placing a suspension of mycelial fragments on a hydrophobic surface in a humid environment at 25℃ for 24h. The pathogenicity assay on rice was performed by spraying 5 ml conidial suspension (5×104 spores/ml) on 15-day-old plants (46). Post-spraying inoculated plants were kept in a sealed chamber with a 90% relative humidity at 25℃ for 24 h. Then, the inoculated plants were removed from the chamber to allow disease symptoms to develop for 4-5 days. The pathogenicity assay on excised barley and rice leaves was performed by cutting a small block from the agar culture of the fungus and placing it on excised leaves for five days in a moist chamber for disease development (68). The sexual reproduction was performed by crossing the tested strain with the sexually compatible strain TH3 on OM plates and then incubating at 19℃ for 30 days with continuous light. The perithecia and clavate asci were photographed in a microscope equipped with a camera (OLYMPUS BX51).

Biomass production for ChIPseq and RNAseq

For ChIP-seq, MoIsw2-GFP Ku80 were used, and for RNAseq *ΔMoisw2* and *Ku80* were used. The strains were grown on Complete medium 2 (CM2) all quantities L^{-1}: 20X Mineral salts solution 50mL, 1000X Trace element solution 1mL, 1000X vitamin solution 1mL, D-glucose 10g, peptone 2g, casamino acid 1g, yeast extract 1g, pH 6.5. For agar medium add 15g agar. Supplemented with 20×Mineral salts solution(1000mL): NaNO3 120g， KCl 10.4g， MgSO4 7H2O 10.4g， KH2PO4 30.4g and with 1000X Vitamin solution (100mL): Biotin 0.01g, Pyridoxin 0.01g, Thiamine 0.01g, Riboflavin 0.01g, PABA (p-aminobenzoic acid) 0.01g, Nicotinic acid 0.01g and 1000X Trace element (100mL): $ZnSO_4$ $7H_2O$ 2.2g, H_3BO_3 1.1g $MnCl_2$ $4H_2O$ 0.5g, $FeSO_4$ $7H_2O$ 0.5g $CoCl_2$ $6H_2O$ 0.17g, $CuSO_4$ $5H_2O$, Na_2MoO_4 $5H_2O$ 0.15g, EDTA 4Na 5g. The plates were incubated for 4-5 days at 28ºC with alternating light-dark cycles (12/12). Mycelial disks (15-20) were punched out using a cork puncher at the colony's edge. The disks were then transferred to 100 ml CM2 liquid medium and cultured for another 48h with shaking (160 RPM, Constant temperature culture oscillator, ZHWY-2102C, Shanghai Zhicheng Analytical Instrument Manufacturing Co., Ltd.). The obtained biomass was filtered using Miracloth, frozen in liquid nitrogen, and sent to the company on dry ice.

ChIP-seq and RNA-seq

Both these techniques were carried out by the company Wuhan IGENEBOOK Biotechnology Co., Ltd, China, according to their method descriptions **(Supplemental Company Methods file**). The last steps about finding motifs and enriched gene classes were carried out differently and is described in this paper. These steps not used are marked in the two method files.

Method for calculating VarR and DelR in the RNAseq data.

We calculated the variability in gene expression for each gene for all the downloaded experimental datasets in the following way. First, we checked that the quality of the data was ok. We have previously found for our own transcriptomic data that a dataset is ok if expressions of genes are rank-ordered then the log log expression of log expression level against the log-rank order should be a smooth downward slightly curved line without big gaps. Also, to be able to compare different sets of data from different experiments the total expression of all genes summed should be similar for all datasets. Next, we calculated the max variation between experiments in the following way. The maximum expression value and the minimum expression value for each gene across the 55 transcriptomes were found. Next, we calculated the average expression for the same data. Finally, we calculated the ratio of maximum expression minus minimum expression divided

by the average expression to arrive at the variation in expression across all experiments for each gene (VarR). In this way any regulation up or down is treated in the same way as access for TFs and repressors to the DNA should be treated equally. Finally comes the problem that some genes had expression values lower than the threshold for detecting them at all (0-values). For these data, we assumed that the expression where at the threshold value instead of 0 and set the expression to that value. In that way, we could include that data without overestimating the VarR for that gene.

The effect of the *MoISW2* mutation (DelR) was estimated in the following way: For each gene we calculated the 2Log ratio of the expression in the mutant divided by the expression in the background. That results in both negative and positive values. Then these values were squared to arrive at only positive values in a similar way as is done with the least square method for curve fitting to arrive at a better estimate of the deviation from the slope. There were very few genes with no detectable expression so no need for handling zero values more than excluding them.

Note that in this paper, we focus on the expression variation of all genes along the chromosomes. Thus, it is the overall pattern that is important and not the values for a single gene. In none of the methods above we used any method for excluding a gene from the analysis based on an arbitrary threshold of 2 times up or down or any other statistically significant threshold for genes. In consequence the calculated values for a single gene cannot and should not be relied upon even if a general increased regulation of many adjacent genes has reliability.

Additional software and add-ins for MS Excel

Addins for MS Excel: The **Fisher Exact** add-in for MS Excel was downloaded from http://www.obertfamily.com/software/fisherexact.html. **Excel solver** used to fit non-standard equations to data is usually part of MS Excel but must be activated in settings.

Freeware: We used the freeware PAST (Hammer, Harper, and Ryan 2001) version 4.08 (released November 2021) for Reduced Major Axis (RMA) regression analysis to handle errors in both the x and y variables. A simple-to-use but powerful freeware program is available from the University of Oslo, Natural History Museum **https://www.nhm.uio.no/english/research/infrastructure/past/.** For simplicity, the data was handled and entered in MS Excel and then copy-pasted into PAST for analysis. The resulting plots were exported from PAST as SVG vector graphic files to be later translated into other vector graphic file formats.

Websites used for analyses and getting necessary additional data

NCBI: **https://www.ncbi.nlm.nih.gov/** (sequence downloads, blasts, annotations including domain annotations)

BROAD: **ftp://ftp.broadinstitute.org** (download of gene order on supercontigs for the 70-15 strain, 1000 upstream DNA sequences for use in MEME)

MEME: https://meme-suite.org/meme/ (use of MEME and FIMO). (Bailey et al. 2015).

See the supplemental file for MEME settings and complete results (Supplemental Data 2). MEME motif 2 was the one with the most hits and was investigated in detail. This motif2 was used for TOMTOM by using the direct link to TOMTOM using the link from the MEME result, for results see the supplemental file (Supplemental Data 3).

FungiFun2 https://elbe.hki-jena.de/fungifun/fungifun.php (Priebe et al. 2015)

Species**:** *Magnaporthe grisea* 70-15 (synonym for *M. oryzae* 70-15).

Classification ontology: FunCat (contains relevant categories for plant pathogens)

Input IDs: For *M. oryzae* 70-15 the MGG_ codes has to be used.

Advanced settings used**:** Significance level; 0.05. Significance test; Fisher's exact test. Test for; Enrichment or Depletion. Adjustment method; No adjustment. Annotation type, Select also indirectly annotated categories.

These settings using "No adjustment" were used since the purpose was not to get super reliable enriched or depleted categories but to compare several FungiFun runs with different Gene ID sets.

antiSMASH

The complete DNA sequence was downloaded from BROAD. That was then submitted to antiSMASH (Blin et al. 2021) fungal version **https://fungismash.secondarymetabolites.org/#!/start** and run with default parameter settings to find the primary genes predicted to be involved in producing secondary metabolites.

Acknowledgments

Professor Daniel J. Ebbole, Texas A&M University, USA, is thanked since he pointed us to the Supercontig sorted gene file for the strain 70-15 that could be downloaded from the BROAD institute. This file was necessary for the present work. This work was supported by grants from Fujian Provincial Science and Technology Key Project (2022NZ030014) Fujian Natural Science Foundation project (2022J01125).

References

Ågren, Göran I., J. Å. Martin Wetterstedt, and Magnus F. K. Billberger. 2012. "Nutrient Limitation on Terrestrial Plant Growth – Modeling the Interaction between Nitrogen and Phosphorus." *New Phytologist* 194 (4): 953–60. https://doi.org/10.1111/j.1469-8137.2012.04116.x.

Allan, Andrew C., and Richard V. Espley. 2018. "MYBs Drive Novel Consumer Traits in Fruits and Vegetables." *Trends in Plant Science* 23 (8): 693–705. https://doi.org/10.1016/j.tplants.2018.06.001.

Ambawat, Supriya, Poonam Sharma, Neelam R. Yadav, and Ram C. Yadav. 2013. "MYB Transcription Factor Genes as Regulators for Plant Responses: An Overview." *Physiology and Molecular Biology of Plants* 19 (3): 307–21. https://doi.org/10.1007/s12298-013-0179-1.

Andrew, Marion, Reeta Barua, Steven M. Short, and Linda M. Kohn. 2012. "Evidence for a Common Toolbox Based on Necrotrophy in a Fungal Lineage Spanning Necrotrophs, Biotrophs, Endophytes, Host Generalists and Specialists." Edited by Jason E. Stajich. *PLoS ONE* 7 (1): e29943. https://doi.org/10.1371/journal.pone.0029943.

Bailey, Timothy L., James Johnson, Charles E. Grant, and William S. Noble. 2015. "The MEME Suite." *Nucleic Acids Research* 43 (W1): W39–49. https://doi.org/10.1093/nar/gkv416.

Baldoni, Elena, Annamaria Genga, and Eleonora Cominelli. 2015. "Plant MYB Transcription Factors: Their Role in Drought Response Mechanisms." *Int. J. Mol. Sci.*, 41.

Bao, Jiandong, Meilian Chen, Zhenhui Zhong, Wei Tang, Lianyu Lin, Xingtan Zhang, Haolang Jiang, et al. 2017. "PacBio Sequencing Reveals Transposable Elements as a Key Contributor to Genomic Plasticity and Virulence Variation in Magnaporthe Oryzae." *Molecular Plant* 10 (11): 1465–68. https://doi.org/10.1016/j.molp.2017.08.008.

Bard, Jonathan BL. 2011. "The next Evolutionary Synthesis: From Lamarck and Darwin to Genomic Variation and Systems Biology." *Cell Communication and Signaling* 9 (1): 30. https://doi.org/10.1186/1478-811X-9-30.

Berdalet, Elisa, Mikel Latasa, and Marta Estrada. 1994. "Effects of Nitrogen and Phosphorus Starvation on Nucleic Acid and Protein Content of *Heterocapsa* Sp." *Journal of Plankton Research* 16 (4): 303–16. https://doi.org/10.1093/plankt/16.4.303.

Blin, Kai, Simon Shaw, Alexander M Kloosterman, Zach Charlop-Powers, Gilles P van Wezel, Marnix H Medema, and Tilmann Weber. 2021. "antiSMASH 6.0: Improving Cluster Detection and Comparison Capabilities." *Nucleic Acids Research* 49 (W1): W29–35. https://doi.org/10.1093/nar/gkab335.

Bourras, Salim, Kaitlin E. McNally, Marion C. Müller, Thomas Wicker, and Beat Keller. 2016. "Avirulence Genes in Cereal Powdery Mildews: The Gene-for-Gene Hypothesis 2.0." *Frontiers in Plant Science* 7 (March). https://doi.org/10.3389/fpls.2016.00241.

Cao, Yiyang, Jia Chen, Xuze Xie, Shenghua Liu, Yue Jiang, Mengtian Pei, Qianfei Wu, et al. 2022. "Characterization of Two Infection-induced Transcription Factors of *Magnaporthe Oryzae* Reveals Their Roles in Regulating Early Infection and Effector Expression." *Molecular Plant Pathology* 23 (8): 1200–1213. https://doi.org/10.1111/mpp.13224.

Cao, Yunpeng, Kui Li, Yanli Li, Xiaopei Zhao, and Lihu Wang. 2020. "MYB Transcription Factors as Regulators of Secondary Metabolism in Plants." *Biology* 9 (3): 61. https://doi.org/10.3390/biology9030061.

Chadha, Sonia, and Mradul Sharma. 2014. "Transposable Elements as Stress Adaptive Capacitors Induce Genomic Instability in Fungal Pathogen Magnaporthe Oryzae." Edited by Kap-Hoon Han. *PLoS ONE* 9 (4): e94415. https://doi.org/10.1371/journal.pone.0094415.

Cheetham, Seth W., Geoffrey J. Faulkner, and Marcel E. Dinger. 2020. "Overcoming Challenges and Dogmas to Understand the Functions of Pseudogenes." *Nature Reviews Genetics* 21 (3): 191–201. https://doi.org/10.1038/s41576-019-0196-1.

Chowdhury, Supriyo, Arpita Basu, and Surekha Kundu. 2017. "Biotrophy-Necrotrophy Switch in Pathogen Evoke Differential Response in Resistant and Susceptible Sesame Involving Multiple Signaling Pathways at Different Phases." *Scientific Reports* 7 (1): 17251. https://doi.org/10.1038/s41598-017-17248-7.

Collemare, Jérôme, Mikaël Pianfetti, Anne-Elodie Houlle, Damien Morin, Laurent Camborde, Marie-Josèphe Gagey, Crystel Barbisan, Isabelle Fudal, Marc-Henri Lebrun, and Heidi U. Böhnert.

2008. "*Magnaporthe Grisea* Avirulence Gene *ACE1* Belongs to an Infection-specific Gene Cluster Involved in Secondary Metabolism." *New Phytologist* 179 (1): 196–208. https://doi.org/10.1111/j.1469-8137.2008.02459.x.

Cutter, Amber R., and Jeffrey J. Hayes. 2015. "A Brief Review of Nucleosome Structure." *FEBS Letters* 589 (20PartA): 2914–22. https://doi.org/10.1016/j.febslet.2015.05.016.

Dang, Weiwei, George L. Sutphin, Jean A. Dorsey, Gabriel L. Otte, Kajia Cao, Rocco M. Perry, Jennifer J. Wanat, et al. 2014. "Inactivation of Yeast Isw2 Chromatin Remodeling Enzyme Mimics Longevity Effect of Calorie Restriction via Induction of Genotoxic Stress Response." *Cell Metabolism* 19 (6): 952–66. https://doi.org/10.1016/j.cmet.2014.04.004.

Desousa, Brandon R, Kristen Ko Kim, Anthony E Jones, Andréa B Ball, Wei Y Hsieh, Pamela Swain, Danielle H Morrow, et al. 2023. "Calculation of ATP Production Rates Using the Seahorse XF Analyzer." *EMBO Reports*, August, e56380. https://doi.org/10.15252/embr.202256380.

Dioh, Waly, Didier Tharreau, Jean Loup Notteghem, Marc Orbach, and Marc-Henri Lebrun. 2000. "Mapping of Avirulence Genes in the Rice Blast Fungus, *Magnaporthe Grisea* , with RFLP and RAPD Markers." *Molecular Plant-Microbe Interactions*® 13 (2): 217–27. https://doi.org/10.1094/MPMI.2000.13.2.217.

Dong, Yanhan, Ying Li, Miaomiao Zhao, Maofeng Jing, Xinyu Liu, Muxing Liu, Xianxian Guo, et al. 2015. "Global Genome and Transcriptome Analyses of Magnaporthe Oryzae Epidemic Isolate 98-06 Uncover Novel Effectors and Pathogenicity-Related Genes, Revealing Gene Gain and Lose Dynamics in Genome Evolution." Edited by Xiaorong Lin. *PLOS Pathogens* 11 (4): e1004801. https://doi.org/10.1371/journal.ppat.1004801.

Donovan, Drake A, Johnathan G Crandall, Vi N Truong, Abigail L Vaaler, Thomas B Bailey, Devin Dinwiddie, Orion GB Banks, Laura E McKnight, and Jeffrey N McKnight. 2021. "Basis of Specificity for a Conserved and Promiscuous Chromatin Remodeling Protein." *eLife* 10 (February): e64061. https://doi.org/10.7554/eLife.64061.

Du, Hai, Li Zhang, Lei Liu, Xiao-Feng Tang, Wen-Jie Yang, Yan-Min Wu, Yu-Bi Huang, and Yi-Xiong Tang. 2009. "Biochemical and Molecular Characterization of Plant MYB Transcription Factor Family." *Biochemistry (Moscow)* 74 (1): 1–11. https://doi.org/10.1134/S0006297909010015.

Dubos, Christian, Ralf Stracke, Erich Grotewold, Bernd Weisshaar, Cathie Martin, and Loïc Lepiniec. 2010. "MYB Transcription Factors in *Arabidopsis*." *Trends in Plant Science* 15 (10): 573–81. https://doi.org/10.1016/j.tplants.2010.06.005.

Erdel, Fabian, and Karsten Rippe. 2011. "Binding Kinetics of Human ISWI Chromatin-Remodelers to DNA Repair Sites Elucidate Their Target Location Mechanism." *Nucleus* 2 (2): 105–12. https://doi.org/10.4161/nucl.2.2.15209.

Erdel, Fabian, Thomas Schubert, Caroline Marth, Gernot Längst, and Karsten Rippe. 2010. "Human ISWI Chromatin-Remodeling Complexes Sample Nucleosomes via Transient Binding Reactions and Become Immobilized at Active Sites." *Proceedings of the National Academy of Sciences* 107 (46): 19873–78. https://doi.org/10.1073/pnas.1003438107.

Fazzio, Thomas G., Marnie E. Gelbart, and Toshio Tsukiyama. 2005. "Two Distinct Mechanisms of Chromatin Interaction by the Isw2 Chromatin Remodeling Complex In Vivo." *Molecular and Cellular Biology* 25 (21): 9165–74. https://doi.org/10.1128/MCB.25.21.9165-9174.2005.

Feurtey, Alice, Cécile Lorrain, Megan C. McDonald, Andrew Milgate, Peter S. Solomon, Rachael Warren, Guido Puccetti, et al. 2023. "A Thousand-Genome Panel Retraces the Global Spread and Adaptation of a Major Fungal Crop Pathogen." *Nature Communications* 14 (1): 1059. https://doi.org/10.1038/s41467-023-36674-y.

Fijarczyk, Anna, Pauline Hessenauer, Richard C. Hamelin, and Christian R. Landry. 2022. "Lifestyles Shape Genome Size and Gene Content in Fungal Pathogens." BioRxiv. https://doi.org/10.1101/2022.08.24.505148.

Ganapathiraju, Madhavi K., Sandeep Subramanian, Srilakshmi Chaparala, and Kalyani B. Karunakaran. 2020. "A Reference Catalog of DNA Palindromes in the Human Genome and Their Variations in 1000 Genomes." *Human Genome Variation* 7 (1): 40. https://doi.org/10.1038/s41439-020-00127-5.

Gostinčar, Cene, Metka Lenassi, Nina Gunde-Cimerman, and Ana Plemenitaš. 2011. "Fungal Adaptation to Extremely High Salt Concentrations." In *Advances in Applied Microbiology*, 77:71–96. Elsevier. https://doi.org/10.1016/B978-0-12-387044-5.00003-0.

Hada, Arjan, Swetansu K. Hota, Jie Luo, Yuan-chi Lin, Seyit Kale, Alexey K. Shaytan, Saurabh K. Bhardwaj, et al. 2019. "Histone Octamer Structure Is Altered Early in ISW2 ATP-Dependent Nucleosome Remodeling." *Cell Reports* 28 (1): 282-294.e6. https://doi.org/10.1016/j.celrep.2019.05.106.

Hammer, Oyvind, David A T Harper, and Paul D Ryan. 2001. "PAST: Paleontological Statistics Software Package for Education and Data Analysis" 4 (1): 9.

Holde, Kensal E. van. 1989. *Chromatin*. Springer Series in Molecular Biology. New York, NY: Springer New York. https://doi.org/10.1007/978-1-4612-3490-6.

Hopfner, Karl-Peter, Christian-Benedikt Gerhold, Kristina Lakomek, and Petra Wollmann. 2012. "Swi2/Snf2 Remodelers: Hybrid Views on Hybrid Molecular Machines." *Current Opinion in Structural Biology* 22 (2): 225–33. https://doi.org/10.1016/j.sbi.2012.02.007.

Hota, Swetansu K., and Blaine Bartholomew. 2011. "Diversity of Operation in ATP-Dependent Chromatin Remodelers." *Biochimica et Biophysica Acta (BBA) - Gene Regulatory Mechanisms* 1809 (9): 476–87. https://doi.org/10.1016/j.bbagrm.2011.05.007.

Huang, Lianggang, Xuejie Li, Liangbo Dong, Bin Wang, and Li Pan. 2021. "Profiling of Chromatin Accessibility Identifies Transcription Factor Binding Sites across the Genome of Aspergillus Species." *BMC Biology* 19 (1): 189. https://doi.org/10.1186/s12915-021-01114-0.

Ipcho, Simon, Thomas Sundelin, Gitte Erbs, H. Corby Kistler, Mari-Anne Newman, and Stefan Olsson. 2016. "Fungal Innate Immunity Induced by Bacterial Microbe-Associated Molecular Patterns (MAMPs)." *G3; Genes|Genomes|Genetics* 6 (6): 1585–95. https://doi.org/10.1534/g3.116.027987.

Jones, Jonathan D. G., and Jeffery L. Dangl. 2006. "The Plant Immune System." *Nature* 444 (7117): 323–29. https://doi.org/10.1038/nature05286.

Josefsen, Lone, Aida Droce, Teis Esben Sondergaard, Jens Laurids Sørensen, Jörg Bormann, Wilhelm Schäfer, Henriette Giese, and Stefan Olsson. 2012. "Autophagy Provides Nutrients for Nonassimilating Fungal Structures and Is Necessary for Plant Colonization but Not for Infection in the Necrotrophic Plant Pathogen Fusarium Graminearum." *Autophagy* 8 (3): 326–37.

Kagalwala, Mohamedi N, Benjamin J Glaus, Weiwei Dang, Martin Zofall, and Blaine Bartholomew. 2004. "Topography of the ISW2–Nucleosome Complex: Insights into Nucleosome Spacing and Chromatin Remodeling." *The EMBO Journal* 23 (10): 2092–2104. https://doi.org/10.1038/sj.emboj.7600220.

Kim, Yongsoo, Hun Kim, Hokyoung Son, Gyung Ja Choi, Jin-Cheol Kim, and Yin-Won Lee. 2014. "MYT3, A Myb-Like Transcription Factor, Affects Fungal Development and Pathogenicity of Fusarium Graminearum." Edited by Jae-Hyuk Yu. *PLoS ONE* 9 (4): e94359. https://doi.org/10.1371/journal.pone.0094359.

Klevecz, R. R., J. Bolen, G. Forrest, and D. B. Murray. 2004. "A Genomewide Oscillation in Transcription Gates DNA Replication and Cell Cycle." *Proceedings of the National Academy of Sciences* 101 (5): 1200–1205. https://doi.org/10.1073/pnas.0306490101.

Kou, Yanjun, Jiehua Qiu, and Zeng Tao. 2019. "Every Coin Has Two Sides: Reactive Oxygen Species during Rice–*Magnaporthe Oryzae* Interaction." *International Journal of Molecular Sciences* 20 (5): 1191. https://doi.org/10.3390/ijms20051191.

Kremer, Stefan C., Stefan Linquist, Brent Saylor, Tyler A. Elliott, T. Ryan Gregory, and Karl Cottenie. 2020. "Transposable Element Persistence via Potential Genome-Level Ecosystem Engineering." *BMC Genomics* 21 (1): 367. https://doi.org/10.1186/s12864-020-6763-1.

Li, H., J. Lu, X. Liu, L. Xhang, and F. Lin. 2012. "Vector Building and Usage for Gene Knockout, Protein Expression and Fluorescent Fusion Protein in The Rice Blast Fungus." *Journal of Agricultural Biotechnology* 20 (1): 94–104. https://doi.org/10.3969/j.issn.1674-7968.2012.01.013.

Li, Jinlu, Guoliang Han, Cuifeng Sun, and Na Sui. 2019. "Research Advances of MYB Transcription Factors in Plant Stress Resistance and Breeding." *Plant Signaling & Behavior* 14 (8): 1613131. https://doi.org/10.1080/15592324.2019.1613131.

Li, Ya, Xiaofeng Yue, Yawei Que, Xia Yan, Zhonghua Ma, Nicholas J. Talbot, and Zhengyi Wang. 2014. "Characterisation of Four LIM Protein-Encoding Genes Involved in Infection-Related Development

958 and Pathogenicity by the Rice Blast Fungus Magnaporthe Oryzae." Edited by Chaoyang Xue. *PLoS*
959 *ONE* 9 (2): e88246. https://doi.org/10.1371/journal.pone.0088246.
960 Li, Yanan, Han Gong, Pan Wang, Yu Zhu, Hongling Peng, Yajuan Cui, Heng Li, Jing Liu, and Zi Wang.
961 2021. "The Emerging Role of ISWI Chromatin Remodeling Complexes in Cancer." *Journal of*
962 *Experimental & Clinical Cancer Research* 40 (1): 346. https://doi.org/10.1186/s13046-021-02151-x.
963 Lin, Yang, Hokyoung Son, Jungkwan Lee, Kyunghun Min, Gyung Ja Choi, Jin-Cheol Kim, and Yin-Won
964 Lee. 2011. "A Putative Transcription Factor MYT1 Is Required for Female Fertility in the
965 Ascomycete Gibberella Zeae." Edited by Jae-Hyuk Yu. *PLoS ONE* 6 (10): e25586.
966 https://doi.org/10.1371/journal.pone.0025586.
967 Lin, Yang, Hokyoung Son, Kyunghun Min, Jungkwan Lee, Gyung Ja Choi, Jin-Cheol Kim, and Yin-Won
968 Lee. 2012. "A Putative Transcription Factor MYT2 Regulates Perithecium Size in the Ascomycete
969 Gibberella Zeae." Edited by Jae-Hyuk Yu. *PLoS ONE* 7 (5): e37859.
970 https://doi.org/10.1371/journal.pone.0037859.
971 Linheiro, Raquel S., and Casey M. Bergman. 2008. "Testing the Palindromic Target Site Model for DNA
972 Transposon Insertion Using the Drosophila Melanogaster P-Element." *Nucleic Acids Research* 36
973 (19): 6199–6208. https://doi.org/10.1093/nar/gkn563.
974 Liu, Jingying, Anne Osbourn, and Pengda Ma. 2015. "MYB Transcription Factors as Regulators of
975 Phenylpropanoid Metabolism in Plants." *Molecular Plant* 8 (5): 689–708.
976 https://doi.org/10.1016/j.molp.2015.03.012.
977 Ma, Dawei, and C. Peter Constabel. 2019. "MYB Repressors as Regulators of Phenylpropanoid Metabolism
978 in Plants." *Trends in Plant Science* 24 (3): 275–89. https://doi.org/10.1016/j.tplants.2018.12.003.
979 Machné, Rainer, and Douglas B. Murray. 2012. "The Yin and Yang of Yeast Transcription: Elements of a
980 Global Feedback System between Metabolism and Chromatin." Edited by Valdur Saks. *PLoS ONE* 7
981 (6): e37906. https://doi.org/10.1371/journal.pone.0037906.
982 Mateos, Laura, Alberto Jiménez, José L. Revuelta, and María A. Santos. 2006. "Purine Biosynthesis,
983 Riboflavin Production, and Trophic-Phase Span Are Controlled by a Myb-Related Transcription
984 Factor in the Fungus *Ashbya Gossypii*." *Applied and Environmental Microbiology* 72 (7): 5052–60.
985 https://doi.org/10.1128/AEM.00424-06.
986 Matheis, S., A. Yemelin, D. Scheps, K. Andresen, S. Jacob, E. Thines, and A.J. Foster. 2017. "Functions of
987 the Magnaporthe Oryzae Flb3p and Flb4p Transcription Factors in the Regulation of Conidiation."
988 *Microbiological Research* 196 (March): 106–17. https://doi.org/10.1016/j.micres.2016.12.010.
989 Menardo, Fabrizio, Coraline R. Praz, Thomas Wicker, and Beat Keller. 2017. "Rapid Turnover of Effectors
990 in Grass Powdery Mildew (Blumeria Graminis)." *BMC Evolutionary Biology* 17 (1): 223.
991 https://doi.org/10.1186/s12862-017-1064-2.
992 Mitra, Partha. 2018. "Transcription Regulation of MYB: A Potential and Novel Therapeutic Target in
993 Cancer." *Annals of Translational Medicine* 6 (22): 443–443.
994 https://doi.org/10.21037/atm.2018.09.62.
995 Mittal, Priya, and Charles W. M. Roberts. 2020. "The SWI/SNF Complex in Cancer — Biology, Biomarkers
996 and Therapy." *Nature Reviews Clinical Oncology* 17 (7): 435–48. https://doi.org/10.1038/s41571-
997 020-0357-3.
998 Monroe, J. Grey, Thanvi Srikant, Pablo Carbonell-Bejerano, Claude Becker, Mariele Lensink, Moises
999 Exposito-Alonso, Marie Klein, et al. 2022. "Mutation Bias Reflects Natural Selection in Arabidopsis
000 Thaliana." *Nature* 602 (7895): 101–5. https://doi.org/10.1038/s41586-021-04269-6.
001 Packer, Michael S., and David R. Liu. 2015. "Methods for the Directed Evolution of Proteins." *Nature*
002 *Reviews Genetics* 16 (7): 379–94. https://doi.org/10.1038/nrg3927.
003 Palloix, A., V. Ayme, and B. Moury. 2009. "Durability of Plant Major Resistance Genes to Pathogens
004 Depends on the Genetic Background, Experimental Evidence and Consequences for Breeding
005 Strategies." *New Phytologist* 183 (1): 190–99. https://doi.org/10.1111/j.1469-8137.2009.02827.x.
006 Pattabiraman, D R, and T J Gonda. 2013. "Role and Potential for Therapeutic Targeting of MYB in
007 Leukemia." *Leukemia* 27 (2): 269–77. https://doi.org/10.1038/leu.2012.225.
008 Pfeiffer, Thomas, and Annabel Morley. 2014. "An Evolutionary Perspective on the Crabtree Effect."
009 *Frontiers in Molecular Biosciences* 1 (October). https://doi.org/10.3389/fmolb.2014.00017.

Piontkivska, Helen, Alejandro P. Rooney, and Masatoshi Nei. 2002. "Purifying Selection and Birth-and-Death Evolution in the Histone H4 Gene Family." *Molecular Biology and Evolution* 19 (5): 689–97. https://doi.org/10.1093/oxfordjournals.molbev.a004127.

Priebe, S., C. Kreisel, F. Horn, R. Guthke, and J. Linde. 2015. "FungiFun2: A Comprehensive Online Resource for Systematic Analysis of Gene Lists from Fungal Species." *Bioinformatics* 31 (3): 445–46. https://doi.org/10.1093/bioinformatics/btu627.

Prouse, Michael B., and Malcolm M. Campbell. 2012. "The Interaction Between MYB Proteins and Their Target DNA Binding Sites." *Biochimica et Biophysica Acta (BBA) - Gene Regulatory Mechanisms* 1819 (1): 67–77. https://doi.org/10.1016/j.bbagrm.2011.10.010.

Rajarammohan, Sivasubramanian. 2021. "Redefining Plant-Necrotroph Interactions: The Thin Line Between Hemibiotrophs and Necrotrophs." *Frontiers in Microbiology* 12 (April): 673518. https://doi.org/10.3389/fmicb.2021.673518.

Reisman, D, S Glaros, and E A Thompson. 2009. "The SWI/SNF Complex and Cancer." *Oncogene* 28 (14): 1653–68. https://doi.org/10.1038/onc.2009.4.

Roy, Sujit. 2016. "Function of MYB Domain Transcription Factors in Abiotic Stress and Epigenetic Control of Stress Response in Plant Genome." *Plant Signaling & Behavior* 11 (1): e1117723. https://doi.org/10.1080/15592324.2015.1117723.

Serrano, Lourdes, Berta N Vazquez, and Jay Tischfield. 2013. "Chromatin Structure, Pluripotency and Differentiation." *Experimental Biology and Medicine* 238 (3): 259–70. https://doi.org/10.1177/1535370213480718.

Smale, Stephen T. 2012. "Transcriptional Regulation in the Innate Immune System." *Current Opinion in Immunology* 24 (1): 51–57. https://doi.org/10.1016/j.coi.2011.12.008.

Song, Zhongshu, Walid Bakeer, James W. Marshall, Ahmed A. Yakasai, Rozida Mohd Khalid, Jerome Collemare, Elizabeth Skellam, et al. 2015. "Heterologous Expression of the Avirulence Gene ACE1 from the Fungal Rice Pathogen Magnaporthe Oryzae." *Chemical Science* 6 (8): 4837–45. https://doi.org/10.1039/C4SC03707C.

Stanton, Kimmy A, Patrick P Edger, Joshua R Puzey, Taliesin Kinser, Philip Cheng, Daniel M Vernon, Nancy R Forsthoefel, and Arielle M Cooley. 2017. "A Whole-Transcriptome Approach to Evaluating Reference Genes for Quantitative Gene Expression Studies: A Case Study in *Mimulus*." *G3 Genes|Genomes|Genetics* 7 (4): 1085–95. https://doi.org/10.1534/g3.116.038075.

Svetec Miklenić, Marina, and Ivan Krešimir Svetec. 2021. "Palindromes in DNA—A Risk for Genome Stability and Implications in Cancer." *International Journal of Molecular Sciences* 22 (6): 2840. https://doi.org/10.3390/ijms22062840.

Toyotome, Takahito, and Katsuhiko Kamei. 2021. "In Vitro Assay of Translation Inhibition by Trichothecenes Using a Commercially Available System." *Toxins* 13 (10): 696. https://doi.org/10.3390/toxins13100696.

Tsukiyama, T., J. Palmer, C. C. Landel, J. Shiloach, and C. Wu. 1999. "Characterization of the Imitation Switch Subfamily of ATP-Dependent Chromatin-Remodeling Factors in Saccharomyces Cerevisiae." *Genes & Development* 13 (6): 686–97. https://doi.org/10.1101/gad.13.6.686.

Valsecchi, Isabel, Özlem Sarikaya-Bayram, Joanne Wong Sak Hoi, Laetitia Muszkieta, John Gibbons, Marie-Christine Prevost, Adeline Mallet, et al. 2017. "MybA, a Transcription Factor Involved in Conidiation and Conidial Viability of the Human Pathogen *Aspergillus Fumigatus*: A Transcription Factor Regulating Conidiation in *Aspergillus*." *Molecular Microbiology* 105 (6): 880–900. https://doi.org/10.1111/mmi.13744.

Verma, Sandhya, Rajesh K. Gazara, and Praveen K. Verma. 2017. "Transcription Factor Repertoire of Necrotrophic Fungal Phytopathogen *Ascochyta Rabiei*: Predominance of MYB Transcription Factors As Potential Regulators of Secretome." *Frontiers in Plant Science* 8 (June): 1037. https://doi.org/10.3389/fpls.2017.01037.

Villalba, F., J. Collemare, P. Landraud, K. Lambou, V. Brozek, B. Cirer, D. Morin, C. Bruel, R. Beffa, and M-H. Lebrun. 2008. "Improved Gene Targeting in Magnaporthe Grisea by Inactivation of MgKU80 Required for Non-Homologous End Joining." *Fungal Genetics and Biology* 45 (1): 68–75. https://doi.org/10.1016/j.fgb.2007.06.006.

062 Wang, X., N. Angelis, and S. L. Thein. 2018. "MYB – A Regulatory Factor in Hematopoiesis." *Gene* 665
063 (July): 6–17. https://doi.org/10.1016/j.gene.2018.04.065.
064 Whitehouse, Iestyn, Oliver J. Rando, Jeff Delrow, and Toshio Tsukiyama. 2007. "Chromatin Remodelling at
065 Promoters Suppresses Antisense Transcription." *Nature* 450 (7172): 1031–35.
066 https://doi.org/10.1038/nature06391.
067 Wieser, Jenny, and Thomas H Adams. 1995. "*fibD* Encodes a Myb-like DNA-Binding Protein That
068 Coordinates Initiation of *Aspergillus Mdulans* Conidiophore Development." *Genes & Development* 9:
069 491–502.
070 Willcockson, Michael A., Sean E. Healton, Cary N. Weiss, Boris A. Bartholdy, Yair Botbol, Laxmi N.
071 Mishra, Dhruv S. Sidhwani, et al. 2021. "H1 Histones Control the Epigenetic Landscape by Local
072 Chromatin Compaction." *Nature* 589 (7841): 293–98. https://doi.org/10.1038/s41586-020-3032-z.
073 Yoshida, Kentaro, Diane G. O. Saunders, Chikako Mitsuoka, Satoshi Natsume, Shunichi Kosugi, Hiromasa
074 Saitoh, Yoshihiro Inoue, et al. 2016. "Host Specialization of the Blast Fungus Magnaporthe Oryzae
075 Is Associated with Dynamic Gain and Loss of Genes Linked to Transposable Elements." *BMC*
076 *Genomics* 17 (1): 370. https://doi.org/10.1186/s12864-016-2690-6.
077 Zhang, Lianhu, Dongmei Zhang, Dan Liu, Yuan Li, Hongchen Li, Yuman Xie, Zonghua Wang, Bjoern Oest
078 Hansen, and Stefan Olsson. 2019. "Conserved Eukaryotic Kinase CK2 Chaperone Intrinsically
079 Disordered Protein Interactions." Edited by Irina S. Druzhinina. *Applied and Environmental*
080 *Microbiology* 86 (2): e02191-19, /aem/86/2/AEM.02191-19.atom.
081 https://doi.org/10.1128/AEM.02191-19.
082 Zhao, Chunzhao, Cees Waalwijk, Pierre JGM de Wit, Dingzhong Tang, and Theo van der Lee. 2014.
083 "Relocation of Genes Generates Non-Conserved Chromosomal Segments in Fusarium
084 Graminearumthat Show Distinct and Co-Regulated Gene Expression Patterns." *BMC Genomics* 15
085 (1): 191. https://doi.org/10.1186/1471-2164-15-191.
086 Zofall, Martin, Jim Persinger, and Blaine Bartholomew. 2004. "Functional Role of Extranucleosomal DNA
087 and the Entry Site of the Nucleosome in Chromatin Remodeling by ISW2." *Molecular and Cellular*
088 *Biology* 24 (22): 10047–57. https://doi.org/10.1128/MCB.24.22.10047-10057.2004.
089
090

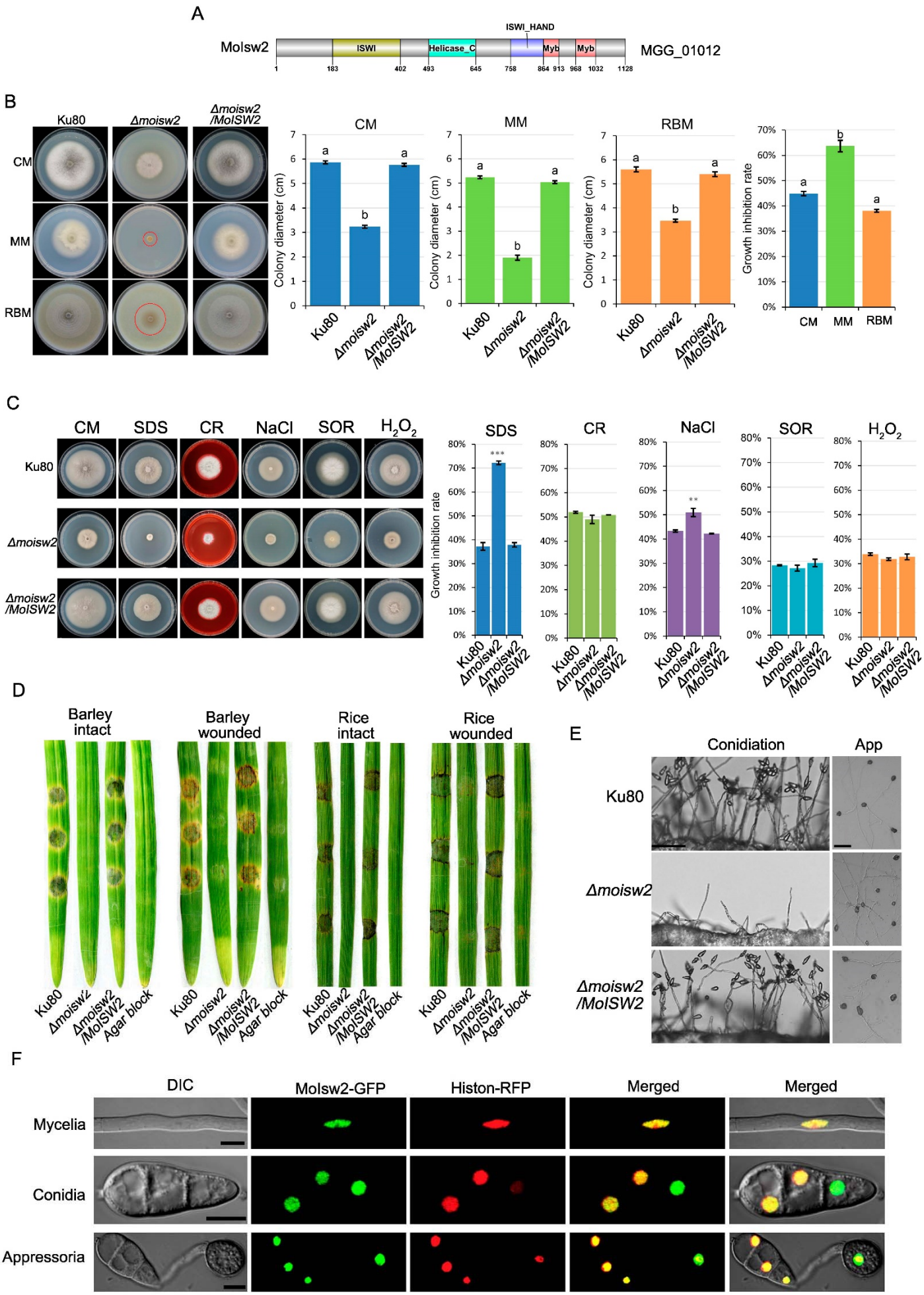
A
MoIsw2
ISWI
Helicase_C
ISWI_HAND
Myb
Myb
MGG_01012
1
183
402
493
645
758
864
913
968
1032
1128
B
Ku80
Δmoisw2
Δmoisw2 /MoISW2
CM
MM
RBM
Colony diameter (cm)
Growth inhibition rate
C
CM
SDS
CR
NaCl
SOR
H2O2
Ku80
Δmoisw2
Δmoisw2 /MoISW2
D
Barley intact
Barley wounded
Rice intact
Rice wounded
Agar block
E
Conidiation
App
F
DIC
MoIsw2-GFP
Histon-RFP
Merged
Merged
Mycelia
Conidia
Appressoria

Figure 1. Domain structure, knockout phenotypes compared to the background Ku80, and localization of MoIsw2. (A) Domain structure (B) Growth phenotypes and growth on complete medium (CM) minimal medium (MM) and rice bran medium (RBM). (C) Stress phenotypes on complete medium (CM) with added Sodium Dodecyl Sulfate (SDS), Congo Red (CR), salt (NaCl), sorbitol (SOR) or hydrogen peroxide (H_2O_2). (D) Infection phenotypes on barley and rice leaves. (E) Conidia formation and appressoria formation from hyphae. (F) Subcellular localization in mycelia, conidia and appressoria MoIsw2-GFP localizes to nuclei (Histon1-RFP nuclear marker). The same letter on the bars indicates $P_{same} >$ *0.05. The stars above bars indicate significant differences from the Ku80 controls ** $P_{same} < 0.01$ ***$P_{same} < 0.001$.

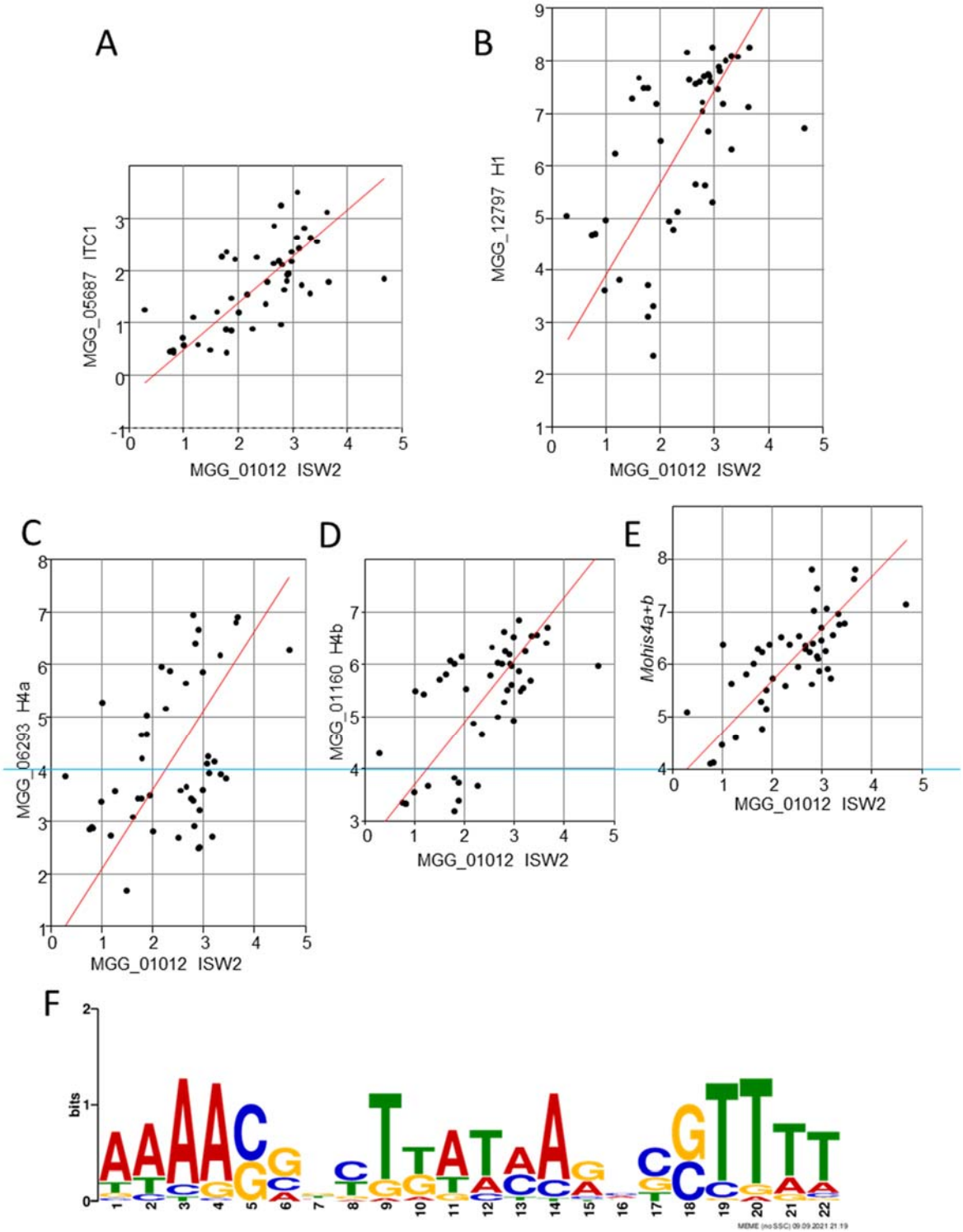

Figure 2. Log2 Reduced Major Axis (RMA) correlations of a putative *ITC1*, the linker histone *HIS1* and the two putative *HIS4* genes putatively expressing the same protein known to interact with the expression of the putative *MoISW2* (x-axis) in published RNAseq data at different stages of plant infection. Each dot represents the two genes' expression in a separate RNAseq dataset. RMA fitting was used to handle the problem of errors in both X and Y axis values, an inherent consequence of plotting the expression of 2 genes against each other. Each dot corresponds to the value from one transcriptome. (**A**) ITC1, P(uncorrelated)=1.57E-7 (**B**) *HIS1*, P(uncorrelated)=1.48E-5 (**C**) *HIS4a* P(uncorrelated)=0.0044 (**D**) *HIS4b* P(uncorrelated)=3.81E-7 (**E**) *HIS4a + 4b* since both *HIS4* genes are predicted to encode for exactly the same protein, P(uncorrelated) 5.82e-10. All plots are shown with equal x and y scale gradings so that it is easy to compare slopes between graphs visually. Also, note that figures **C**, **D**, and **E** have been positioned so that Log 4 on the Y-axes are on the same line so that the effect of the addition, Log2(His4a+His4b), can be seen visually. (**F**) A frequently occurring palindromic motif was found in the ChIP-seq data using MoIsw2 as bait. It was found in 196 sequences.

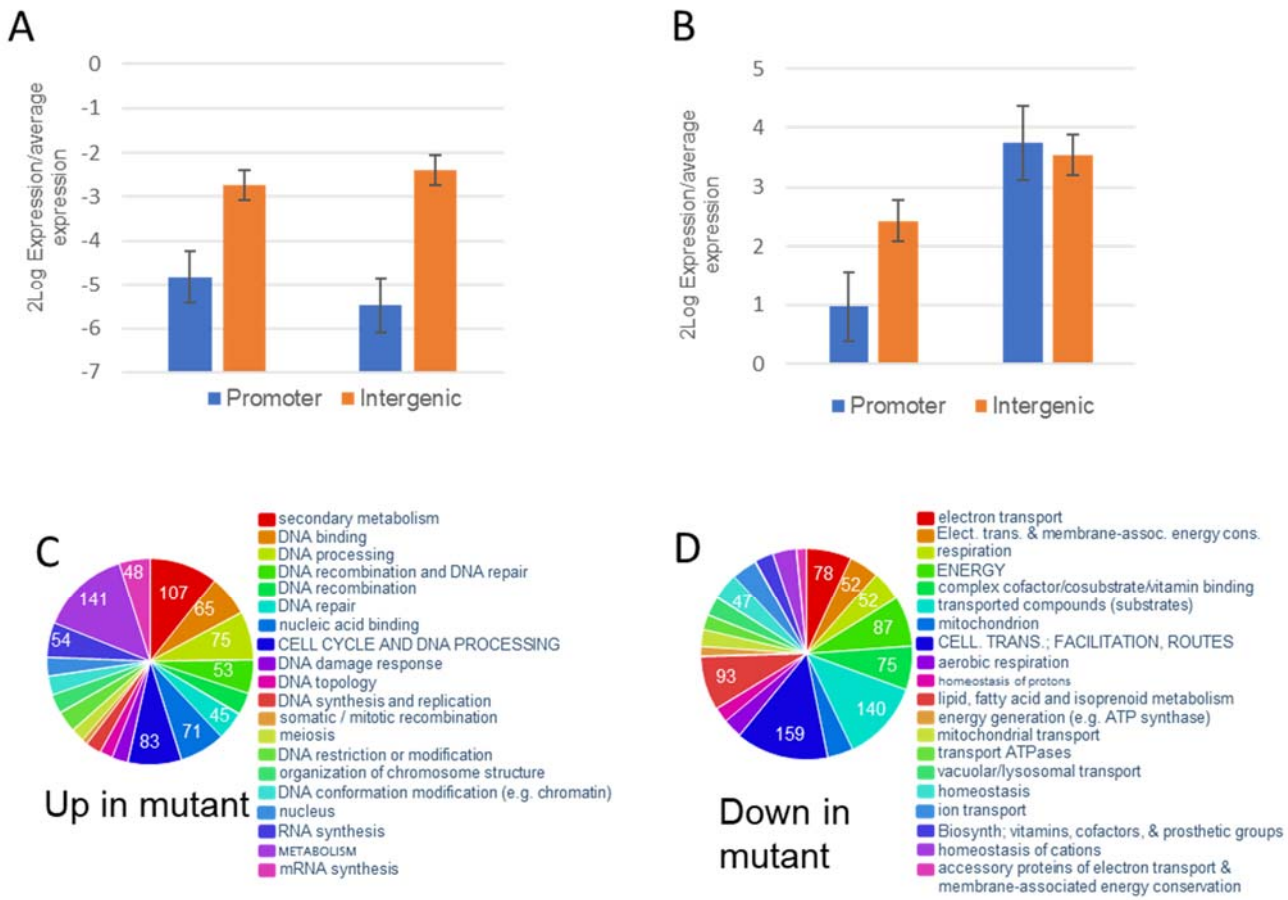

Figure 3. Deletion-induced change in expression of genes next to the predicted palindromic MoIsw2 DNA binding site with hits for the MoIsw2 binding in the ChIP-seq data compared to the average regulation of all genes. (**A**) Expression was, on average higher of genes closest to the binding site in *ΔMoISW2* than Ku80, or with the motif in their promoter region. (**B**) Expression of genes with a binding site in the promoter region and the closest gene when MoIsw2 binding is intergenic. MoIsw2 upregulates both gene types and upregulates genes slightly further away from the binding site, while the absolute (plus or minus) regulation is equal for both types of genes (8-16 times regulation). Error bars indicate SEM (Promoter N=63 Intergenic N=112). (**C**) 20 most significantly enriched upregulated FunCat gene categories in the *ΔMoISW2* compared to the background strain Ku80; Secondary metabolism, DNA-binding, and genes for DNA-related activities and synthesis (anabolism). (**D**) 20 Significantly enriched downregulated genes in the mutant are genes for, mitochondrial activities like electron transport and mitochondrial biosynthesis, respiration, transport routes (catabolism).

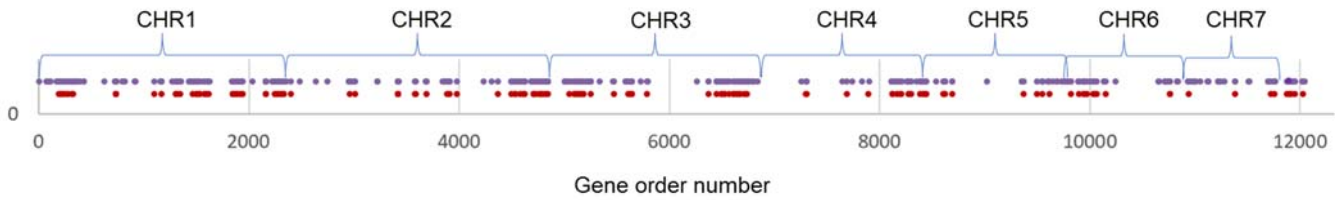

Figure 4. The position of TEs and identified palindromic MoIsw2 binding sites in DNA largely overlaps along the whole genome.

Table 1. Comparison of the position of avirulence genes in relation to the MoIsw2 palindromic DNA binding motif sites in strain Guy11, as well as differential regulation between experiments of the avirulence genes in MoISW2 knockout compared to the background, and differential regulation of the same genes during infection of rice in strain Guy11, and strain 98-06 from published data. Blue-marked cells; are genes that MoIsw2 help regulate in only in Guy11. Green-marked cells; are genes that are only regulated during infection by 98-06. DelR and VarR contains variation in expression in RNAseq data between mutant and Ku80, and between 55 downloade RNAseq datasets from different labs, repectively (see text below for explanation of these measures). Several of the listed avirulence genes are not present in any of the two strain and some are only present in one of them.

ID.	Annotation	Distance from the closest gene to MoIsw2 binding site Guy11	DelR Guy11	Guy11 expr (X)	98-06 expr (X)	VarR Guy11
MGG_12447	cytochalasan	0	19.31	X		48.20
MGG_08386	cytochalasan	NP				
MGG_08377	cytochalasan	NP				
MGG_08378	cytochalasan	1	15.25	X		15.25
MGG_08380	cytochalasan	?			X	
MGG_08381	cytochalasan	?			X	
MGG_08384	cytochalasan	2	0.08	X	X	**29.55**
MGG_08389	cytochalasan	2	2.33	X	X	**24.59**
MGG_08390	cytochalasan	1	0.00	X	X	**56.00**
MGG_08391	cytochalasan	?			X	
MGG_15927	cytochalasan	?			X	
MGG_15928	cytochalasan	NP				
	Avirulence genes					
MGG_07199	ATR13, RxLR effector	170	0.04	X	X	7.27
MGG_10556	Avr_Pii	NP				
MGG_17614	Avr_Pii	NP				
MGG_13283	Avr_Pik	NP				
MGG_15972	Avr_Pik	?			X	
MGG_03029	Avr_Pita1	175	37.08			19.74
MGG_07038	Avr_Pita1	169	2.00			6.25
MGG_09617	Avr_Pita1	NP				
MGG_10927	Avr_Pita1	20	0.07			**24.00**
MGG_03808	Avr_Pita1 like	NP				
MGG_15370	Avr_Pita1 like	1	0.28			**56.00**
MGG_17611	Avr_Pita1	NP				
MGG_14981	AVR_PiTA2	NP				
MGG_15212	AVR_Pita2	?			X	
MGG_18041	Avr_Piz-t	NP				
MGG_03685	Avr-Pi54	238	14.11			3.86
MGG_13863	Avr-PWL1	?			X	
MGG_07398	Avr-PWL2	NP		X		
Sum number	30			7	11	
Only in one of the strains				3	7	
				In both		
				4		

NP=Not Present in Guy11 or 98-06

Bold numbers=Seem to be more important during plant infection

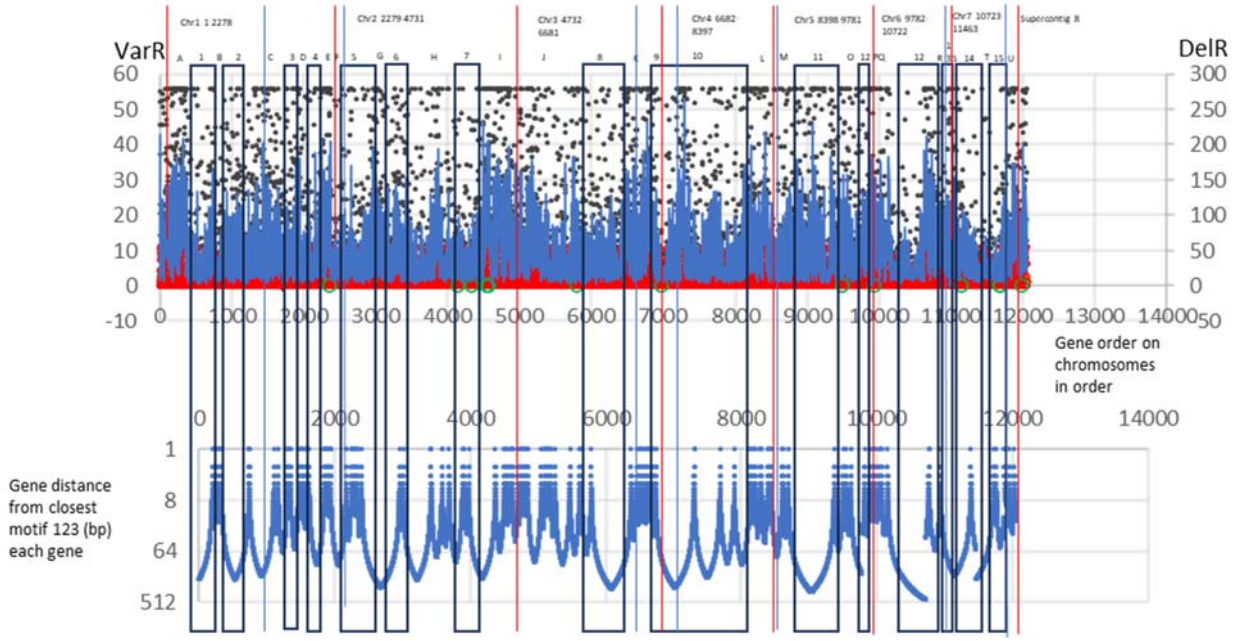

Figure 5. Plot of distances of all genes to closest motifs 123 motifs (**bottom**) in relation to plot of variation of expression across 55 downloaded RNAseq experiments (black points and blue 5 point moving average) combined with difference in gene expression between the *MoISW2* mutant and the Ku80 background (Red points and bright red 5 point moving average (**top**). For the VarR data Several genes had at least one condition when their expression were below the detection level while otherwise expressed in these cases the gene expression were set to the lowest detected gene expression. That creates the line of black dots at the top of the top figure. The density of the line of dots (top figure) together with areas with less than 16 gene distances from the motif sites paints out the regions of the genome with most variation in both the VarR and DelR data. The genome contains A-U genomic regions with high variability of gene expression close (less than 16 genes away) to the MoIsw2 123 DNA binding motifs sites and 1-15 regions with lower variation. Note bottom Y axis is log and reverse, X axis is order on chromosomes in chromosome order for the whole genome to get genome order.

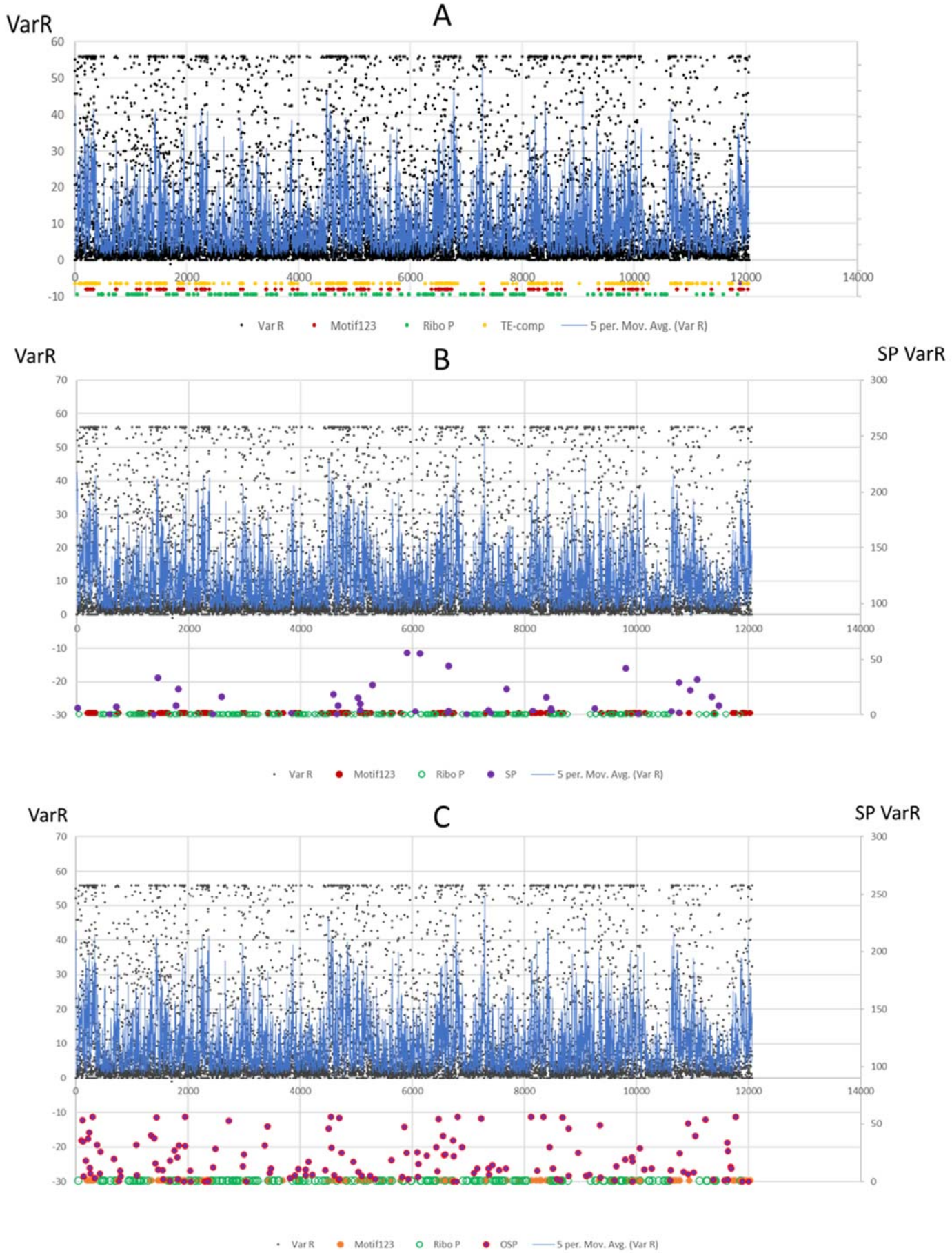

Figure 6. Position of housekeeping ribosomal genes and genes encoding secreted proteins in relation to the MoIsw2 DNA binding motifs a genes encoding ribosomal genes in relation to VarR variability. (**A**) Ribosomal genes. (**B**) Genes

80 for secreted proteins (SP) with conserved domains (generally larger proteins). (**C**) Genes for other secreted proteins
81 (OSP) without any conserved domains identified (generally small proteins).
82

.

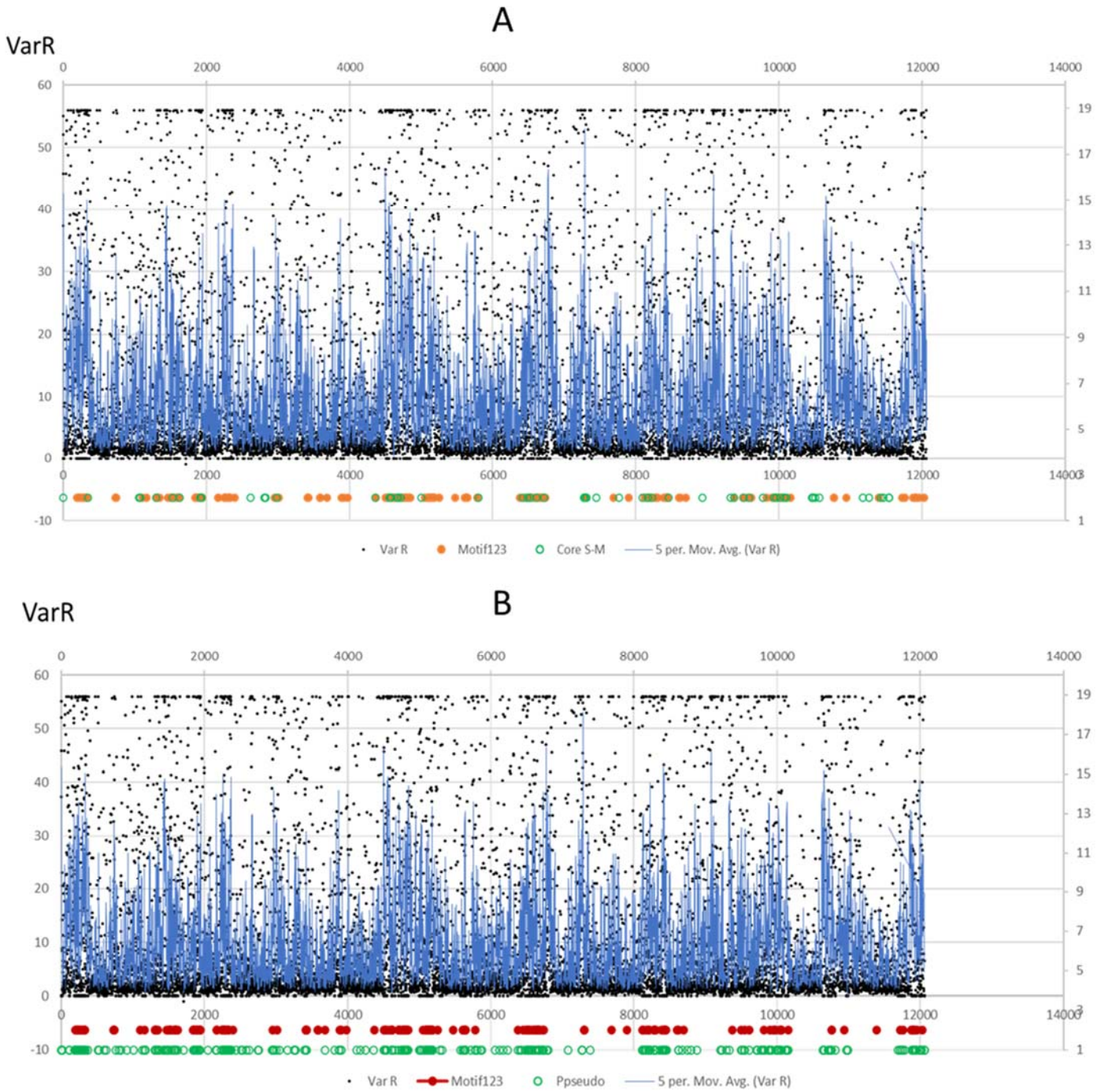

Figure 7. Position of core econdary metabolite genes and potential pseudogenes in relation to the MoIsw2 DNA binding motifs and genes encoding ribosomal genes in relation to VarR variability. (**A**) Core secondary metabolite genes (green rings). (**B**) Potential pseudogenes not expressed in any treatment (dark green rings). In both A and B the positions of the 123 MoIsw2 DNA binding sites are marked as references.

Table 2. Annotation of the 65 DNA binding genes identified in the analysis shown in Fig. 3C. These genes are the most upregulated in *ΔMoISW2* compared to the expression in the background Ku80-strain. Annotation from NCBI. Note: these are the genes that are most repressed by the MoIsw2 activity.

MGG_02762	MGG_02762. ATP-dependent RNA helicase DED1; Belongs to the DEAD box helicase family
MGG_06470	MGG_06470, DNA repair helicase RAD25 (835 aa).
MGG_05948	MGG_05948 zinc knuckle domain-containing protein. This domain is a zinc-binding domain of the form CxxCxxxGHxxxxC from various species. It is found in the MPE1 protein from Saccharomyces cerevisiae which is a component of the cleavage and polyadenylation factor (CPF) complex important for polyadenylation-dependent pre-mRNA 3'-end formation
MGG_01990	b-ZIP transcription factor IDI-4 (induces autophagic cell death in the fungus *Podospora*)
MGG_00868	Global Transactivator; Superfamily II DNA or RNA helicase, SNF2 family [Transcription, Replication, recombination and repair];
MGG_02429	KOG4062 6-O-methylguanine-DNA methyltransferase MGMT/MGT1, involved in DNA repair Replication, recombination and repair https://jgi-myco-web-4.jgi.doe.gov/annotator/servlet/jgi.annotation.Annotation?pDb=Lasov1&pStateVar=View&pProteinId=680852&pViewType=protein
MGG_07015	DNA repair protein Rad7
MGG_11518	G/U mismatch-specific uracil DNA glycosylase
MGG_04428	Zinc finger transcription factor ace1
MGG_07118	sporulation-specific protein 5 (needed for sexual spore formation?)
MGG_05995	MGG_05995, Magnaporthe oryzae 70-15 hypothetical protein (244 aa), translin family protein, Translin family (PF01997). If Translin, here is a review about that https://link.springer.com/article/10.1007/s12038-019-9947-6.
MGG_04429	ATP-dependent DNA helicase MPH1; ATP-dependent DNA helicase is involved in DNA damage repair by homologous recombination and genome maintenance.

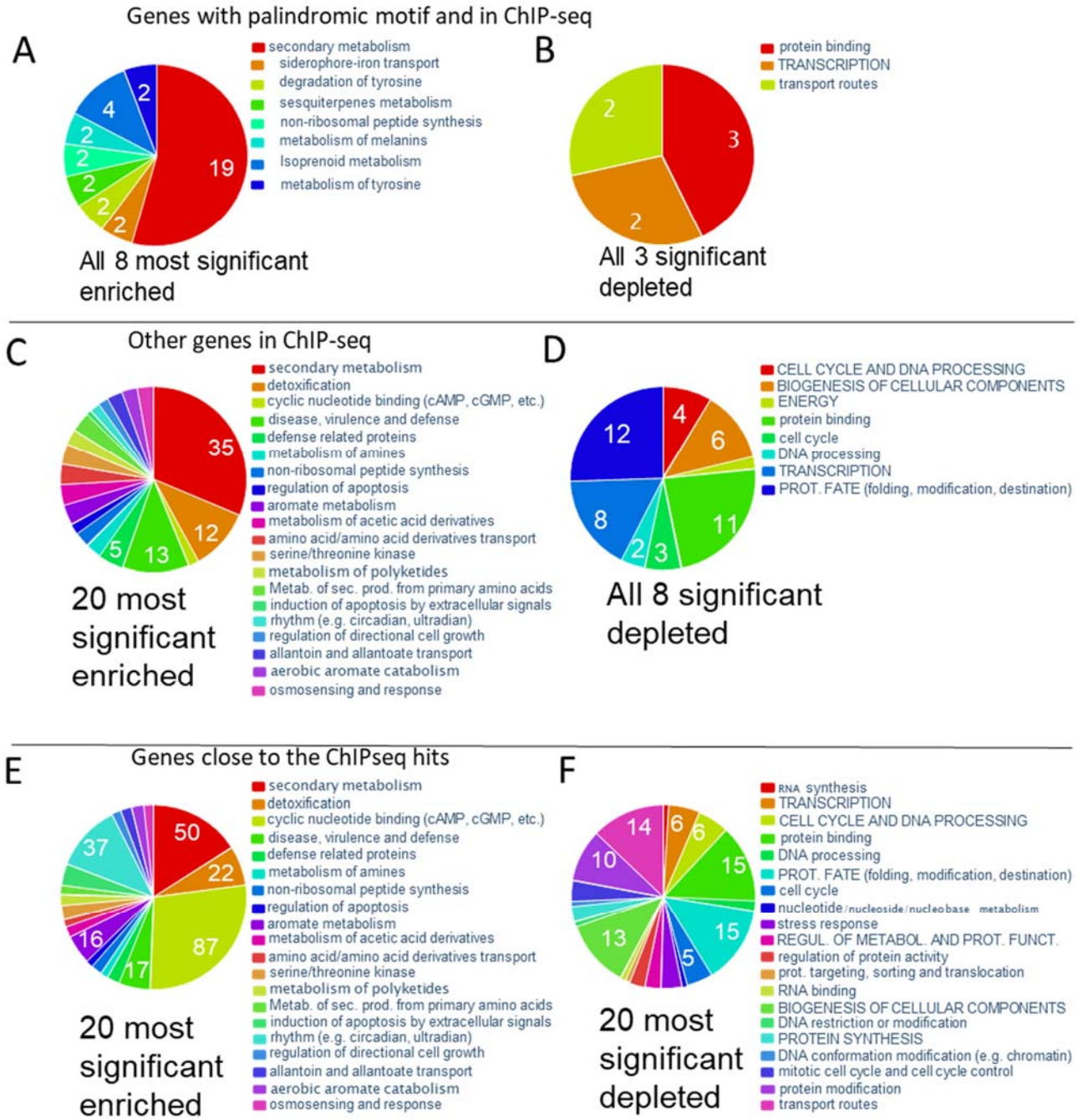

Figure 8. FunCat classification of genes at or close to the MoIsw2 DNA binding sites. (**A**) Significantly enriched and depleted classes of genes in the MoIsw2 ChIP-seq binding assay that also has the MoIsw2 DNA-binding palindromic motif in their upstream region. **(B)** Significantly enriched and depleted classes of all genes with ChIP-seq sequences with MoIsw2 binding to their upstream regulatory DNA sequences. **(C)** Significantly enriched and depleted classes of genes closest to intergenic hits (excluding the palindromic motif hits) for MoIsw2 binding.

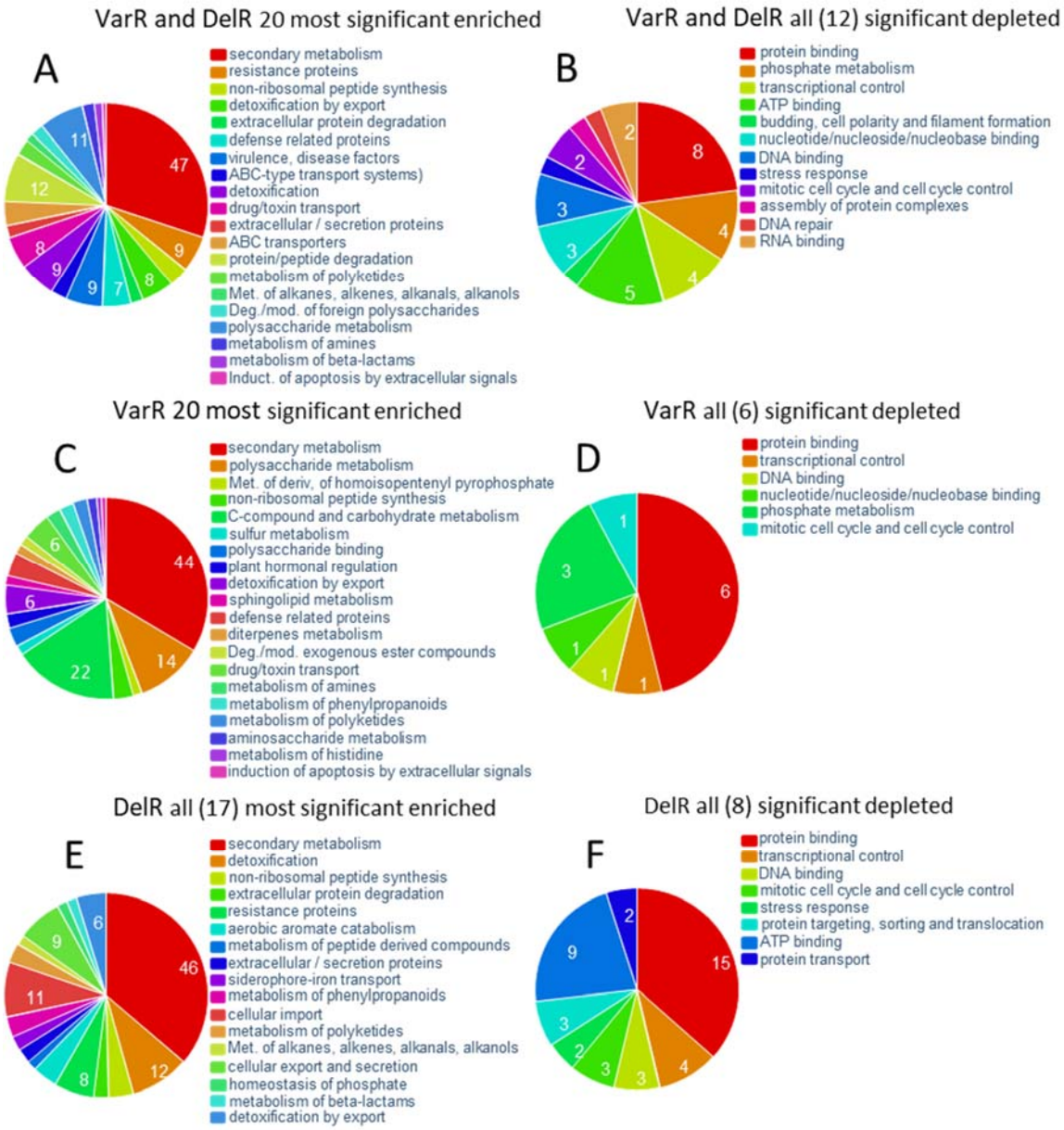

Figure 9. FunCat classification of 500 genes with most variable gene expression between experiments. (**A**) VarR and DelR enriched. (**B**) VarR and DelR depleted. (**C**) VarR alone Enriched. (**D**) VarR alone depleted. (**E**) DelR alone enriched. (**F**) DelR alone depleted.

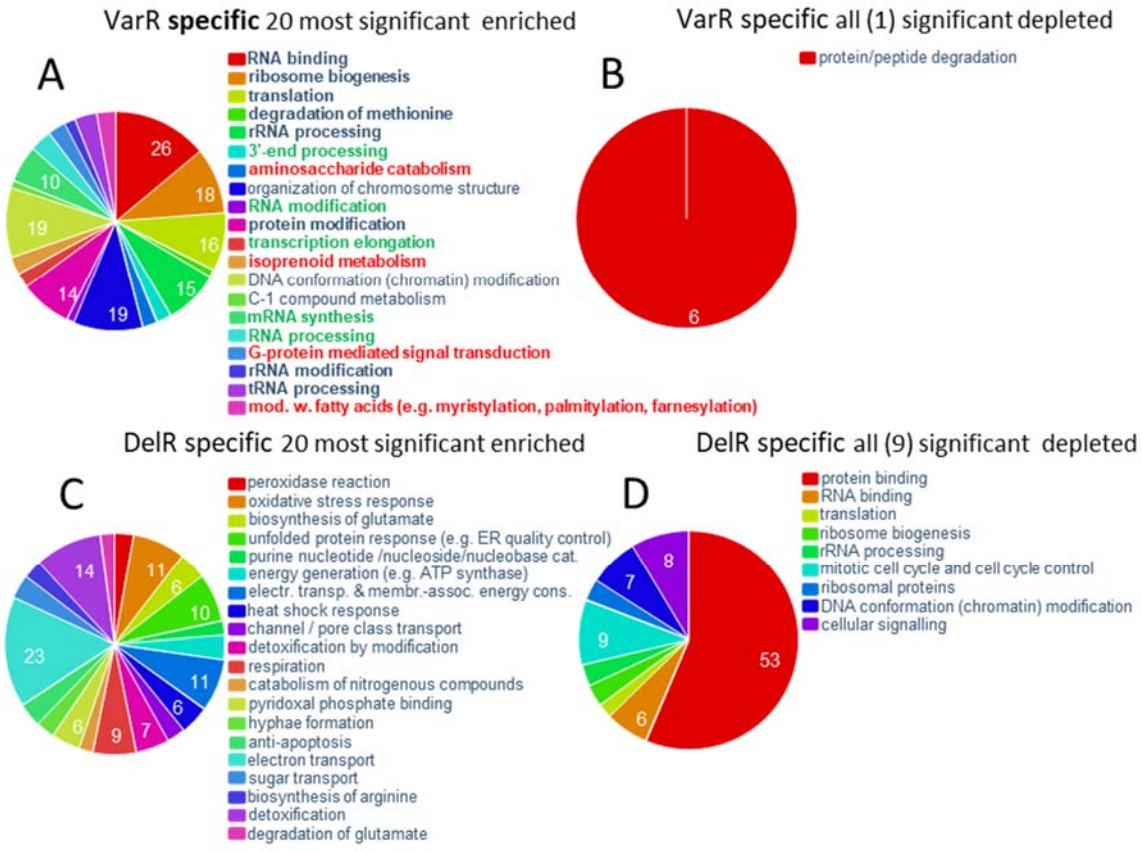

Black bold=translation related
Green bold=transcription related
Red bold=innate immunity related (towards plant? amino saccharide metabolism)

Figure 10. Differences between 500 VarR-specific and DelR-**specific** functional gene classes illustrate the difference in conditions between *in planta* experiments and *in vitro* experiments. (**A**) VarR-specific enriched functional gene classes specifically responding *in planta*. Colour-marked texts are the functional gene classes of special interest for plant pathogenicity (see text). (**B**) VarR-specific depleted functional gene classes specifically responding *in planta*. (**C**) DelR-specific enriched functional gene classes specifically responding *in vitro* (**D**) DelR-specific depleted functional gene classes specifically responding *in vitro.*

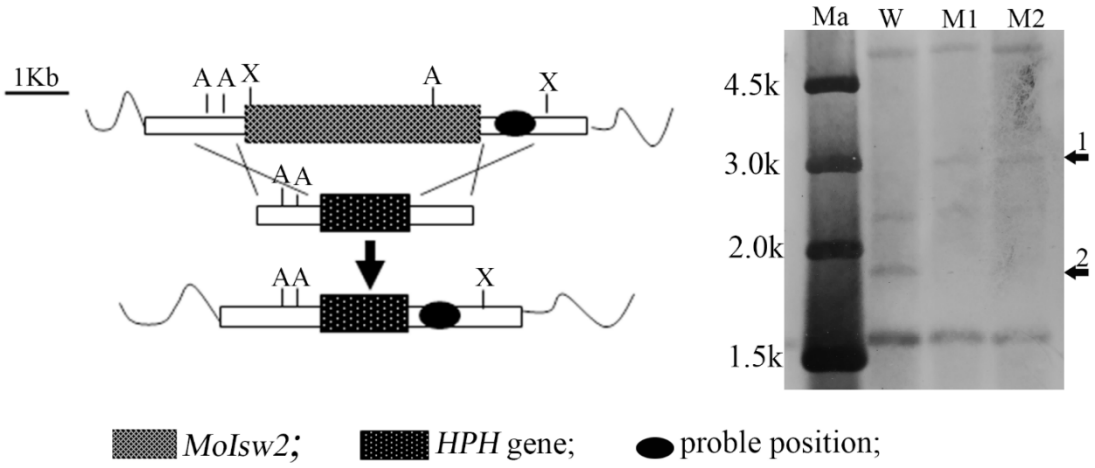

Figure S1. Southern blot confirmation for MoIsw2 mutants. The 1.0 kb downstream of the target gene was used as a probe for blotting. The arrow1 indicates the expected bands that should be present in mutants. The arrow2 indicates the expected bands that should not be present in the mutants, but present in Wild-type strain. W, Wild-type strain; M1 and M2, two mutants of the target gene; Ma, Mark; A, AgeI; X, XhoI;

Overall statistics
R2: 0,5252
MSE: 0,3663

MANOVA
Wilks´ lambda: 0,3447
F: 41,82
df1: 2
df1: 44
p(regr): 6,669E-11

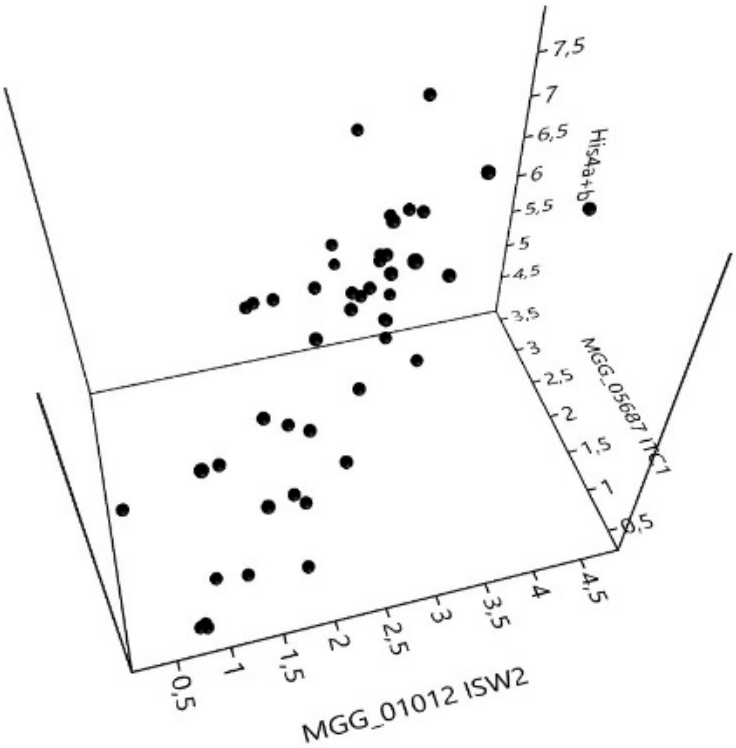

Figure S2. 3D plot showing the Log of expression of *MoISW2*, *MoITC1*, and *MoHIS4a+b* that, according to the literature, need to work together to influence nucleosome packing. They are all correlated and form a nice 3d "sausage" as they should if the three genes encode proteins that need to work together. Multiple regression with *MoISW2* as an independent variable, and *MoITC1*, and *MoHIS4a+b* dependent gives a linear relationship (P=6.7E-11).

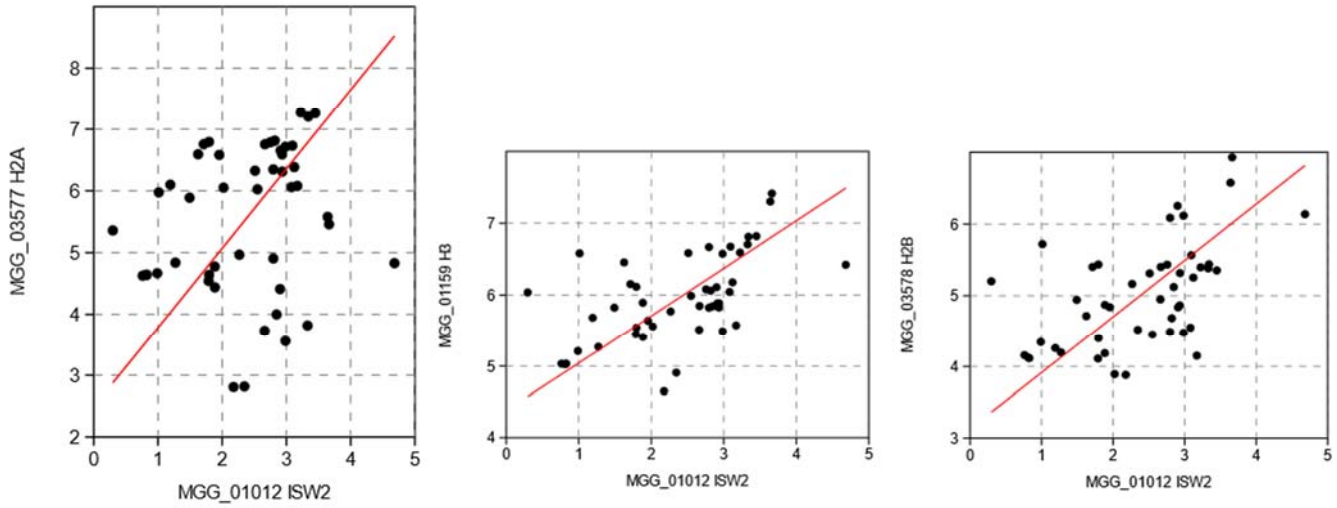

Figure S3. Log2 RMA correlations of a putative *MoHIS2a, MoHIS3* and *MoHIS2B* with the expression of *MoISW2* (x-axis) in published RNAseq data at different stages of plant infection. (**A**) *MoHIS2a*, P(uncorr=0.20 (**B**) *MoHIS3*, P(uncorr)=8.94E-5 (**C**) *MoHIS2B*, P(uncorr)=3.56E-5.

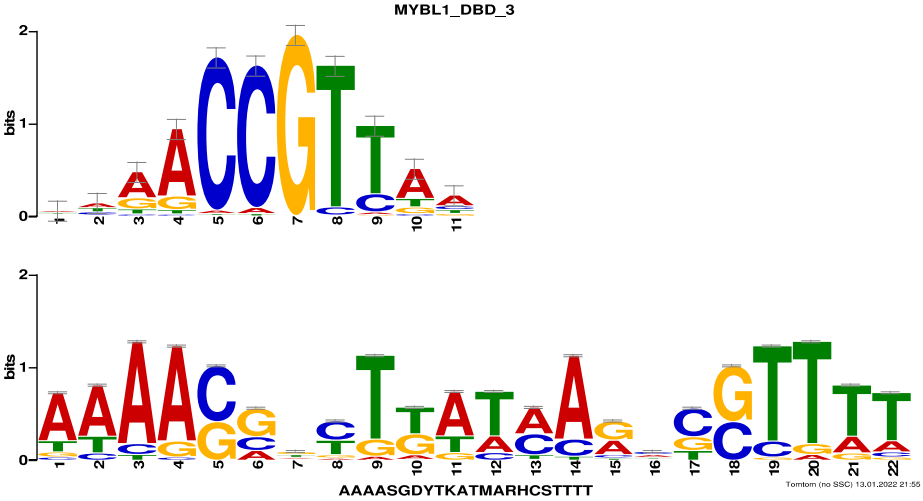

Figure S4. Comparison of the motif (Bottom) with the known human Myb protein DNA binding motif (Top) found by a TOMTOM query using the motif in Fig. 2F as the query. The MoIsw2 DNA binding site has a palindromic Myb/SANT-like DNA binding motif with a similarity to the human protein MYBL1.

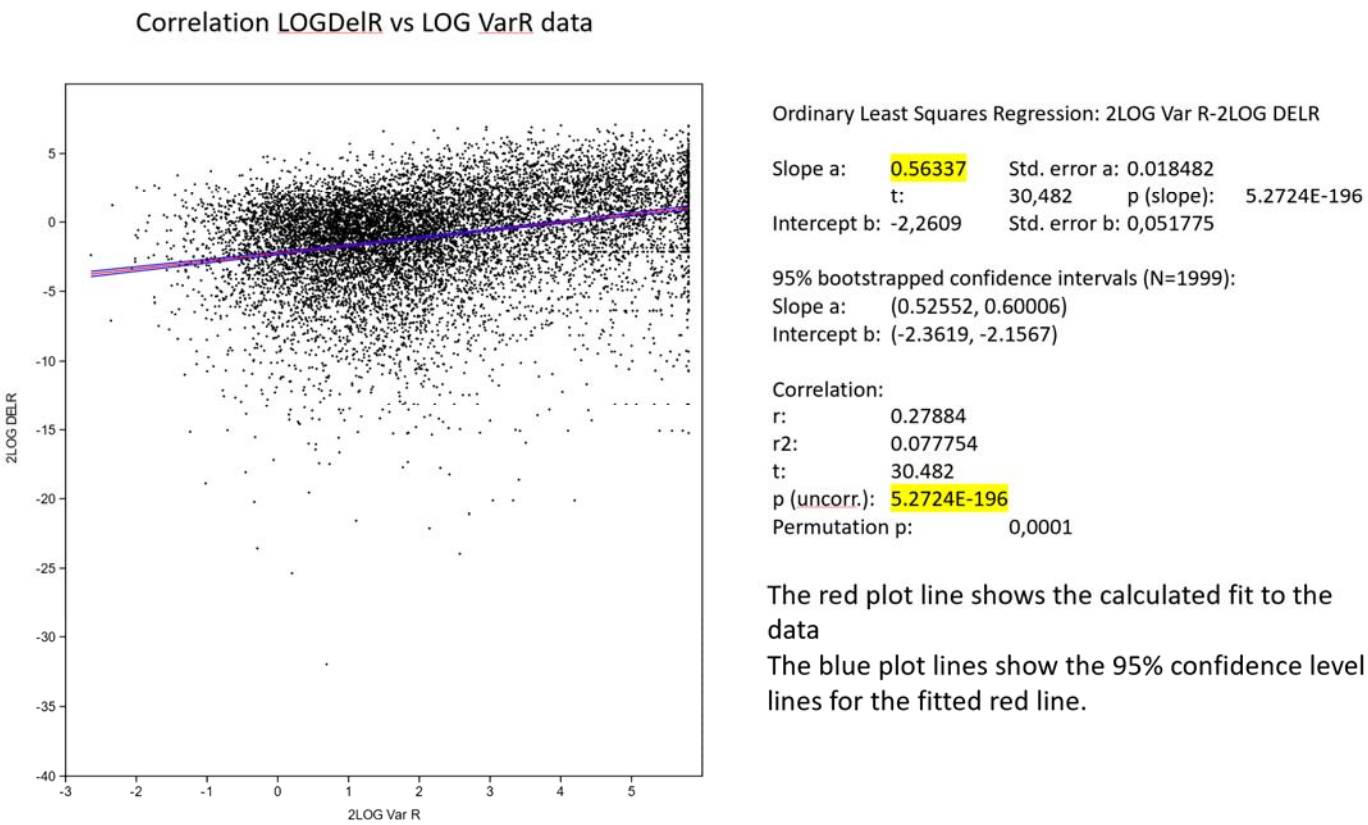

Figure S5 Correlation between 2Log DelR vs 2Log VarR data. The VarR responses in planta and the DelR responses in vitro are correlated. Genes with very low VarR variability are good candidates as reference genes for the *in planta* experiments. Genes with low DelR variability are good candidates for the in vitro experiments. The commonly used reference gene that seemed to show very low variability was the actin gene. The technique should be able to be used to select good and stable reference gene candidates for RNAseq for different conditions. It should be able to find genes stable enough that small changes in the expression of target genes like TFs and other regulators and receptors can be detected since thos gene classes can have large biological effects even with minor expression changes.

Key resources table

REAGENT or RESOURCE	SOURCE	IDENTIFIER
MoISW2GFP	This study	
Critical commercial assays		
ChIP seq service	IGENEBOOK (see this paper supplementa file)	Supplemental Company methods.zip
RNAseq service	IGENEBOOK (see this paper supplemental file)	Supplemental Company methods.zip
Deposited data		
RNAseq compilation of published experiments on gene expressions during infection stages	Zhang et al.[1]	https://doi.org/10.6084/m9.figshare.7068857.v1
ChIPsec data for MoISW2 binding M. oryzae Ku80 DNA RNAseq data for strains ΔMoIsw2 and Ku80 + other supplemental files and analyses 100Mb zip file.	This study	https://figshare.com/s/df7b6b0bf9caf963a06c reserved DOI https://doi.org/10.6084/m9.figshare.22218328
Magnaporthe oryzae genome and genes sequences	BROAD institute	ftp.broadinstitute.org/distribution/annotation/fungi/magnaporthe/genomes/magnaporthe_oryzae_70-15_8 User: Anonymous
Magnaporth oryzae expression Avir genes during rice infection. Strain 98-06	Cao et al. [2]	https://bsppjournals.onlinelibrary.wiley.com/action/downloadSupplement?doi=10.1111%2Fmpp.13224&file=mpp13224-sup-0010-TableS2.xlsx
Transposable elements in M. oryzae and secreted protein gene MGG ID lists.	Bao et al.[3]	https://www.cell.com/cms/10.1016/j.molp.2017.08.008/attachment/1ef9f990-eada-4c84-bd0c-68313587dc7d/mmc1.pdf
Sequence downloads, blasts, annotations including domain annotations	NCBI	https://www.ncbi.nlm.nih.gov/

Experimental models: Organisms/strains		
Magnaporthe oryzae (formerly named *Magnaporthe grisea*)		Ku80[4] deletion in strain Guy11 https://mycocosm.jgi.doe.gov/MagorGY11_1/MagorGY11_1.home.html
MoISW2-GFP strain derived from Ku80	This study	
Software and algorithms		
PAST statistics software package version 4.08 (released November 2021)	Hammer et al.[5]	https://www.nhm.uio.no/english/research/infrastructure/past/
Microsoft Excel (MS Office 365) with Solver Add-In activated	Microsoft	https://www.microsoft.com
Fisher Exact Add-In for MS Excel	software@obertfamily.com	http://www.obertfamily.com/software/fisherexact.html
Other		
FungiFun2 website for Functional Category analysis of putative proteins.	Priebe et al. [6]	https://elbe.hki-jena.de/fungifun/fungifun.php
antiSMASH website for finding core secondary metabolite genes in fungi.	Blin et al. [7]	https://fungismash.secondarymetabolites.org/#!/start
The MEME suite for use of MEME and FIMO	Bailey et al. [8]	https://meme-suite.org/meme/

1. Zhang, L. *et al.* Conserved Eukaryotic Kinase CK2 Chaperone Intrinsically Disordered Protein Interactions. *Appl Environ Microbiol* **86**, e02191-19, /aem/86/2/AEM.02191-19.atom (2019).
2. Cao, Y. *et al.* Characterization of two infection-induced transcription factors of *Magnaporthe oryzae* reveals their roles in regulating early infection and effector expression. *Molecular Plant Pathology* **23**, 1200–1213 (2022).
3. Bao, J. *et al.* PacBio Sequencing Reveals Transposable Elements as a Key Contributor to Genomic Plasticity and Virulence Variation in Magnaporthe oryzae. *Molecular Plant* **10**, 1465–1468 (2017).
4. Villalba, F. *et al.* Improved gene targeting in Magnaporthe grisea by inactivation of MgKU80 required for non-homologous end joining. *Fungal Genetics and Biology* **45**, 68–75 (2008).
5. Hammer, O., Harper, D. A. T. & Ryan, P. D. PAST: Paleontological Statistics Software Package for Education and Data Analysis. **4**, 9 (2001).
6. Priebe, S., Kreisel, C., Horn, F., Guthke, R. & Linde, J. FungiFun2: a comprehensive online resource for systematic analysis of gene lists from fungal species. *Bioinformatics* **31**, 445–446 (2015).
7. Blin, K. *et al.* antiSMASH 6.0: improving cluster detection and comparison capabilities. *Nucleic Acids Research* **49**, W29–W35 (2021).
8. Bailey, T. L., Johnson, J., Grant, C. E. & Noble, W. S. The MEME Suite. *Nucleic Acids Res* **43**, W39–W49 (2015).